

Dust around R Coronae Borealis stars: I. Spitzer/IRS observations

D. A. García-Hernández^{1,2}, N. Kameswara Rao^{3,4}, David L. Lambert⁴

ABSTRACT

Spitzer/IRS spectra from 5 to 37 μm for a complete sample of 31 R Coronae Borealis stars (RCBs) are presented. These spectra are combined with optical and near-infrared photometry of each RCB at maximum light to compile a spectral energy distribution (SED). The SEDs are fitted with blackbody flux distributions and estimates made of the ratio of the infrared flux from circumstellar dust to the flux emitted by the star. Comparisons for 29 of the 31 stars are made with the IRAS fluxes from three decades earlier: Spitzer and IRAS fluxes at 12 μm and 25 μm are essentially equal for all but a minority of the sample. For this minority, the IRAS to Spitzer flux ratio exceeds a factor of three. The outliers are suggested to be stars where formation of a dust cloud or dust puff is a rare event. A single puff ejected prior to the IRAS observations may have been reobserved by Spitzer as a cooler puff at a greater distance from the RCB. RCBs which experience more frequent optical declines have, in general, a circumstellar environment containing puffs subtending a larger solid angle at the star and a quasi-constant infrared flux. Yet, the estimated subtended solid angles and the blackbody temperatures of the dust show a systematic evolution to lower solid angles and cooler temperatures in the interval between IRAS and Spitzer. Dust emission by these RCBs and those in the LMC is similar in terms of total 24 μm luminosity and [8.0]–[24.0] color index.

Subject headings: circumstellar matter — dust, extinction — stars: chemically peculiar — stars: white dwarfs — infrared: stars

¹Instituto de Astrofísica de Canarias, C/ Via Láctea s/n, 38200 La Laguna, Spain; agarcia@iac.es

²Departamento de Astrofísica, Universidad de La Laguna (ULL), E-38205 La Laguna, Spain

³Indian Institute of Astrophysics, Bangalore 560034, India; nkrao@iiap.res.in

⁴W. J. McDonald Observatory. The University of Texas at Austin. 1 University Station, C1400. Austin, TX 78712–0259, USA; dll@astro.as.utexas.edu

1. Introduction

The R Coronae Borealis (here, RCB) stars are notable for two distinct peculiarities (Clayton 1996). First, they are hydrogen-poor, helium-rich supergiants: the H-deficiencies range from about 10-100 to at least 10^8 . Second, the RCB stars experience unpredictable and rapid declines in brightness: declines of 2 to 8 magnitudes in the visual occurring at intervals of less than a year to greater than 20 years last from weeks to months to years. These declines are caused by formation of a cloud of carbon soot above the Earth-facing surface of the star. Discovery of an infrared excess confirmed the obvious suspicion that the stars were dust producers (Stein et al. 1969; Feast et al. 1997). Typical blackbody temperatures of the dust run from about 400 K to 900 K. In a representative case, about one-third of the photospheric flux is absorbed by dust and reemitted in the infrared. The observation that the infrared flux may be little affected by a decline shows that the dust is distributed in clouds around the star (Forrest et al. 1972). Recently, high angular resolution images of RY Sgr, a bright RCB, at 2.2, 4.5, and 8–13 μm showed clearly that the dust is indeed distributed in clouds (de Laverny & Mékarnia 2004; Leão et al. 2007; Bright et al. 2011). IRAS photometry at long wavelengths showed that, in addition to the warm dust, some RCBs have dust at a lower temperature (say, 30 K to 100 K) and, therefore, at large distances from the star (Rao & Nandy 1986; Walker 1986; Gillett et al. 1986).

Each of the two principal peculiarities prompts leading questions. In the case of the H-deficiency, that question is - what are the evolutionary origins of the RCBs that result in a H-poor stars? Two scenarios remain under active consideration for the RCBs and their putative relatives the H-deficient carbon (HdC) stars to lower temperatures and the extreme helium (EHe) stars to higher temperature. In one, the H-poor supergiant is formed from the merger of a He white dwarf with a C-O white dwarf; the double-degenerate (DD) scenario. In the competing picture, the H-poor supergiant results from a final post-AGB shell flash in the central star of a planetary nebula; the so-called final flash (FF) scenario. In both cases, the trigger - the merger or the final flash - transforms a white dwarf into a H-poor supergiant for a period of a few thousand years. There is evidence that both the DD and FF scenarios occur but the DD scenario seems likely to account for the majority of the RCBs.

Several insights into the origins of the RCBs are coming from spectroscopic determinations of the stellar chemical compositions (Lambert & Rao 1994; Asplund et al. 2000; Clayton et al. 2005, 2007; García-Hernández et al. 2009, 2010; Jeffery et al. 2011; Pandey & Lambert 2011). Detailed abundance analyses, which are possible for the warm RCBs but rarely undertaken for the cool RCBs with their spectra rich in molecular lines, suggest that many RCBs are likely fruits of the DD scenario. A few RCBs show several highly unusual abundance signatures and, in particular, very distinctive Si/Fe and S/Fe ratios. Such stars

are called ‘minority’ RCBs - see Lambert & Rao (1994) who introduced the terms ‘majority RCB’ and ‘minority RCB’ star. A rare class of hot RCBs is discussed by De Marco et al. (2002) and includes DY Cen, a minority RCB.

The other principal peculiarity – the unpredictable declines – stimulates a series of questions about the dust around RCB stars such as: What is the composition of the dust? Where does dust form relative to the stellar surface? What triggers formation of the obscuring cloud? How frequently do dust clouds form? Does dust form at preferred latitudes on the star or are formation sites spread uniformly across the stellar surface? Clayton (1996) reviews evidence pertinent to these questions. Perhaps, the key novel theoretical idea of recent times comes from Woitke et al. (1996) who developed a model in which a pulsation-induced shock triggers dust nucleation near the star (one to two stellar radii out) as gas behind the outward propagating shock cools below the condensation temperature (say, < 1500 K) in the star’s upper atmosphere. Presence of cool gas during light minima has now been detected in three RCBs: R CrB (Rao et al. 2006; Rao & Lambert 2010), V854 Cen (Rao & Lambert 2000), and V CrA (Rao & Lambert 2008). Light variations at maximum light are common among RCBs and generally interpreted as arising from pulsations. Absorption line splitting suggestive of an atmospheric shock is regularly observed for RY Sgr (Danziger 1965; Cottrell & Lambert 1982) and occasionally for R CrB. Pugach (1977) noted a correlation between the onset of a light decline for RY Sgr and the pulsation phase. Crause et al. (2007) from long-term photometric studies of four RCBs have shown that a decline occurs at a particular phase of the pulsation cycle, although not every pulsation cycle results in a decline. Thus, evidence is accumulating that dust formation occurs near the star. Radiation pressure on the dust grains is considered to drive them rapidly outward.

Clues to several of the questions concerning the dust are contained in the shape of the infrared continuum emitted by the circumstellar dust, the presence of emission or absorption features imposed on that continuum, and on the temporal variation of the infrared flux. Ground-based infrared spectrophotometry has revealed a smooth continuum in the atmospheric windows; strong emission and absorption features have not been seen. Inability to observe in regions blocked by the Earth’s atmosphere is an especially serious problem in searching for features attributable to dust. Infrared Space Observatory (ISO) spectra obtained for just three (the brightest) RCBs - R CrB, RY Sgr, and V854 Cen - at a resolution of $R=1000$ showed for the first time some excess emission over a quasi-blackbody continuum (Lambert et al. 2001). Broad unidentified emission features were seen centered on about $6 \mu\text{m}$ and $13 \mu\text{m}$. Emission features from $4 \mu\text{m}$ to $15 \mu\text{m}$ for V854 Cen but not for R CrB and RY Sgr showed a resemblance to a laboratory spectrum of hydrogenated amorphous carbon (Colangeli et al. 1995; Scott et al. 1997).

With the advent of the Spitzer Space telescope, it became possible for the first time to extend low-resolution infrared spectroscopy to a much larger sample of RCBs. In this paper, we present a library of infrared Spitzer/IRS spectra for a large sample (31) of RCB stars. Spectra are characterized by a fit of blackbodies to optical and infrared photometry and the Spitzer spectra. Estimates are provided of the infrared flux emitted by dust to the total stellar flux. Comparisons are made with previously reported measurements of the infrared flux, principally the $12\mu\text{m}$ and $25\mu\text{m}$ flux measurements from the IRAS satellite. Infrared emission features superimposed on the blackbody continua will be discussed in detail in a subsequent paper. Emission spectra of DY Cen and V854 Cen showing features from polycyclic aromatic hydrocarbons (PAHs) and C_{60} have been discussed by García-Hernández et al. (2011). Spitzer/IRS spectra of the hot RCB stars V348 Sgr and HV 2671 are presented in Clayton et al. (2011).

Section 2 describes our sample of RCB stars, the Spitzer/IRS and some ground-based photometric observations obtained at about the same time as the Spitzer observations, and the IRAS observations. Section 3 constructs the spectral energy distributions (SEDs) from ~ 0.4 to $38\mu\text{m}$ from optical and infrared observations, where the SEDs are fitted using blackbodies for the star and the dust for each object. Spitzer and IRAS observations are compared and discussed in Section 4, while a comparison of the RCB dust emission in different metallicity environments is offered in Section 5. Finally, the paper concludes with Section 6.

2. The sample and observations

2.1. The RCB sample

Our main goal in obtaining Spitzer observations was to compile a library of infrared spectra for as complete a sample of RCBs as possible. Table 1 list the 31 RCB stars included in this study together with some relevant information such as coordinates, the date of the Spitzer observation, Spitzer program ID, etc. Eighteen RCBs were in our approved GO program. An additional 13 warm RCBs were found in the public Spitzer database. The sample provides comprehensive coverage of the hot RCBs, warm RCBs and includes several of the coolest RCBs. The target list in Table 1 is also identified according to the categories A, B, or C. Category A corresponds to warm RCBs across the composition range (13 stars) where compositions are taken from Asplund et al. (2000). Category B is assigned to the few (5) minority RCB stars. The coolest RCB stars belong to category C (13 stars). Note that minority stars V3795 Sgr, VZ Sgr, V CrA, V854 Cen and DY Cen fall in categories A and B (AB) and Z UMi is assigned to the category BC. The RCB star HV 2671 in the Large

Magellanic Cloud (LMC) has yet to be assigned to one of the categories; De Marco et al. (2002) note that HV 2671 and V348 Sgr have almost identical optical spectra but the Spitzer spectra are very different although HV 2671 shows similarities with V854 Cen (Clayton et al. 2011). Also in Table 1, we indicate whether a star was observed at or below maximum light.

2.2. Spitzer observations

The infrared spectra were taken with the Infrared Spectrograph (IRS, Houck et al. 2004) on board the Spitzer Space Telescope (Werner et al. 2004). We obtained 5.2–37.2 μm spectra for 18 sources in our sample under our General Observer Program (#50212, P.I.: D. L. Lambert) that was carried out between April and October 2008. We used a combination of IRS Short-Low (5.2–14.5 μm ; $64 < R < 128$, here SL), Short-High (9.9–19.6 μm , here SH) and Long-High (18.7–37.2 μm , here LH) observations ($R \sim 600$). Since IRAS fluxes at 12 and 25 μm are available for all sources in our sample, we assumed we had *a priori* knowledge of the mean brightness of each source at the different wavelengths covered by IRS. Most of these sources are very bright (with mid-IR SEDs peaking at $\sim 12 \mu\text{m}$), and two cycles of 6 s in each of the three modules were used. For those sources with lower flux densities at 25 μm , four cycles of 14 s were employed in the LH module. We typically reached a S/N larger than 50 in the SL and SH modules; these modules cover the 5.2–19.5 μm range where most of the spectral features of our interest fall. However, the achieved S/N is generally lower in the LH module. For three stars (those sources brighter than 5.5 Jy at 12 μm ; see Table 1) we did not obtain spectroscopy in the SL module in order to avoid saturation.

IRS spectra for 13 other stars were retrieved from the Spitzer database. These spectra were taken by different observers and using different module combinations (see Table 1). In general, the quality of these spectra is also very good ($S/N \geq 50$); specially when the SL and LL (Long-Low: 14.0–38.0 μm ; $64 < R < 128$) modules are used. The Spitzer/IRS spectra of the infrared-bright RCB stars V854 Cen, RY Sgr and R CrB - previously observed by the ISO satellite (Lambert et al. 2001) - are included in this subgroup.

We retrieved the 1-D infrared spectra processed by the Spitzer data reduction pipeline (versions 15.3.0, 16.1.0, 17.2.0, 18.0.2 and 18.7.0) for all sources in our sample from the Spitzer database. These post-bcd products (one spectra for each nod position) are automatically reduced by the IRS Custom Extractor (SPICE) with a point source aperture. The automatic data reduction includes the extraction from the 2-D images as well as the wavelength and flux calibration. It is to be noted here that for the SL and LL data, the two nod position 2-D images are subtracted in order to cancel out the sky background. However,

for the high-resolution modules no background subtraction is done since no sky measurements were taken; the SH and LH slits are too small for on-slit background subtraction. The Spitzer-contributed software SMART (Higdon et al. 2004) was later used for cleaning of residual bad pixels, spurious jumps and glitches and for smoothing and merging into one final spectrum per source. Note that all sources in our sample are bright point-like objects for which the automatic data reduction pipeline works very well; no significant differences between these spectra and those manually reduced are found.

We found a good match (i.e., better than 5%) between the different modules for approximately half of the sample stars. Most of the rest of stars displayed a very good match between the SL and SH modules, confirming their point-like nature but the LH data showed a flux excess of about 5–20%. We attribute this mismatch to the fact the these LH fluxes are more uncertain and to possible background emission. Indeed, several of these stars are located toward high extinction line of sights (i.e., their infrared spectra are affected by amorphous silicate absorptions from the diffuse interstellar medium; see below). Thus, we applied a correction factor to the LH observations in order to scale them to the SH spectra. It should be noted that only the RCB star VZ Sgr seems to be slightly extended at infrared wavelengths,

Reduced spectra – λF_λ versus λ – are shown in Figure 1-5 for the complete sample of 31 stars.

2.3. Ground-based optical/near-IR photometry

To complement the Spitzer observations, we carried out photometric observations in the optical and near-infrared for some of the sample. Our intention was to ascertain a star’s status (i.e., if the stars were at maximum or minimum light) during the Spitzer observations. However, these “simultaneous” photometric data were obtained only for the 18 RCB stars observed with Spitzer through Program 50212 (Table 2). If a star was at maximum light, the photometry is used in the construction of the spectral energy distribution (SEDs) from the visible to $\sim 40 \mu\text{m}$ in our sample stars. For stars not at maximum light, photometry from the literature was used to establish the stellar energy distribution at maximum light across the optical.

Optical photometry in the Johnson-Bessell V, R, and I filters was obtained with the IAC-80 telescope (Observatorio del Teide, Spain) equipped with the CAMELOT CCD¹ for

¹see e.g., <http://www.iac.es/telescopes/pages/es/inicio/instrumentos/camelot.php>

more details. The observations were done as near as possible to the Spitzer observation dates and sometimes the stars were observed twice (i.e., before and after Spitzer). The VRI magnitudes for each star were derived by using standard aperture photometry tasks in IRAF². The flux calibration was done by using the photometric calibration for CAMELOT³ and making use of standard stars observed on the same night. The use of this average photometric calibration implies that our derived VRI magnitudes are precise to ~ 0.15 mag. This error in the optical magnitudes is more than enough for our purposes, that is, to know the variability status of these RCB stars. Table 2 displays a log of the optical observations done (e.g., the observation dates) together with the VRI photometry for each star observed.

JHKL photometry (Table 2) was obtained at the South African Astrophysical Observatory (SAAO) with the 0.75m telescope by F. Van Wyk at our request. These observations are on the SAAO system using Carter (1990) standards.

3. Spectral Energy Distributions

3.1. Methodology

In this section, we present the spectral energy distribution (SED) from ~ 0.4 to $40 \mu\text{m}$ for each RCB star. UBVR_IJHKLMN magnitudes are converted to fluxes with the magnitude-flux and effective wavelength calibrations taken from Tokunaga (2000). For a majority of the stars, there are UBVR_IJHK magnitudes in the literature. Some data are available for L magnitudes and a few for MN magnitudes. In addition, there are the ground-based measurements in Table 2.

The goal was to construct the ‘stellar’ SED from observations made when the star was at maximum light. This SED uses the UBVR_IJHK fluxes except that for a few stars some observations of K and possibly H are contaminated by emission by dust. In addition to the Spitzer spectrum of the dust emission, we consider the IRAS $12\mu\text{m}$ and $25\mu\text{m}$ measurements and available LMN photometry. The LMN, Spitzer and IRAS fluxes are primarily from the circumstellar dust. As is well known, optical and infrared variability are not tightly coupled - see below and especially Feast et al. (1997).

²Image Reduction and Analysis Facility (IRAF) software is distributed by the National Optical Astronomy Observatories, which is operated by the Association of Universities for Research in Astronomy, Inc., under cooperative agreement with the National Science Foundation.

³see <http://www.iac.es/telescopes/pages/en/home/utilities.php#camelot-calibration> for the average extinction coefficients, color terms, etc.

These SEDs are corrected for interstellar reddening provided by the line of sight to the RCB. Spitzer spectra require a correction for absorptions at $9.7\mu\text{m}$ and $18\mu\text{m}$, attributable to interstellar silicates. For this correction, the reddening curve is adopted from Chiar & Tielens (2006) by taking $A(K)/A(V)=0.114$ (Cardelli et al. 1989) with an extrapolation from 27 to 38 μm assuming the same slope as between 23 to 27 μm . The correction was generally ignored for stars where the predicted reddening was less than about $E(B-V)$ of 0.4. The correction for the $9.7\mu\text{m}$ interstellar absorption can have a particularly strong effect on the profile and intensity of the 6-10 μm emission feature, the subject of a subsequent paper.

A few stars in Table 1 were observed by Spitzer in decline. For these stars, we assemble the stellar SED from published photometry at maximum light; we do not use the contemporary photometry, if available, in Table 2. This is then combined with the Spitzer spectrum to provide that star’s SED which is corrected, as usual, for interstellar reddening.

In the case of the IRAS 12 μm and 25 μm photometry, the measurements were color corrected. Color-corrected flux densities were mostly obtained from Walker (1986). In some cases, measurements in the IRAS Point Source Catalogue were corrected following the prescriptions given by Beichman et al. (1988 - Table VI.C.6).

Each reddening-corrected SED was fitted with a combination of blackbodies with one blackbody at the stellar effective temperature and one or two blackbodies to represent the infrared circumstellar component. In a few cases, a third circumstellar blackbody was considered. Table 3 summarizes the fits by giving the temperature and the estimated flux ratio for the blackbody relative to the stellar flux where $R = f_{cool}/f_{star}$ is referred to as the covering factor. The sum of the R -values for a given star is essentially independent of the assumption that dust emission may be represented by one or more blackbodies. Our R -values do not include the small contribution from the 6-10 μm emission feature. Entries are given for both the Spitzer and IRAS fits except where there is no significant difference between the two fits.

All sources of photometry and interstellar reddening are identified below where brief descriptions are also given of other characteristics of each star (frequency of declines, comparison with IRAS and other IR fluxes, etc.). A primary source on the frequency of declines is Jurcsik (1996) who compiled the inter-fade periods for a majority of our sample. She defines a fading of a RCB to be ‘an initial drop of about 1 mag from a maximum light, independently of the duration and complexity of the minima.’ The AAVSO website provides a historical record of the light curves of many of our RCBs from which we also estimate the frequency of declines. In addition, the ASAS-3⁴ website provides 9 year light curves in the V-band for many stars in our sample, covering the epoch of the Spitzer observations.

⁴See <http://www.astrouw.edu.pl/asas/>

3.2. Individual Stars

UV Cas: UV Cas is very rarely seen in decline. Zavatti (1975) from a sparse data set assembled from the literature found “during 69 years of observations only one deep minimum”, a minimum of about four magnitudes recorded more than eighty years ago. An excellent data set from the AAVSO extending back to the 1950s shows no deep declines in last 60 years. There is evidence for a 1.2 magnitude decline between 1954 August and 1956 August and perhaps one or two even weaker declines but none for the past 30 years. Jurcsik (1996) gives the inter-fade period as 25500 days, among her sample of 27 RCBs only XX Cam at 36000 days fades less frequently.

VRI photometry (Table 2) was obtained at the time of the Spitzer observations. We take UBV photometry from Fernie et al. (1972); the star is only slightly variable in UBV. 2MASS JHK magnitudes are adopted (Cutri et al. 2003). A valuable set of JHKLM photometry from 1984–2009 is provided by Bogdanov et al. (2010).

The Spitzer spectrum shows the interstellar $9.7 \mu\text{m}$ silicate absorption band which is almost entirely removed when the spectrum is corrected assuming $E(B-V) = 0.9$. Rao (1980) estimated $E(B-V)=1.0$ from interstellar reddening maps (Fitzgerald 1968) and the assumption that this luminous star must be beyond the majority of the reddening.

Corrected for interstellar reddening, the UBVRi magnitudes are fitted by a 7200 K blackbody, close to the effective temperature found from optical spectroscopy by Asplund et al. (2000). The 2MASS JHK fluxes imply a brighter blackbody by about 0.2 magnitudes. The Spitzer fluxes are fitted with the principal contribution from a 510 K blackbody and minor contributions from the Planck tail of the stellar blackbody and a colder (180 K) blackbody (Figure 6 – lefthand panel, and Table 3). The covering factor R sums to 0.035 for the two cool blackbodies (Table 3), one of the lowest R for the entire sample. Also, the $6\text{-}10\mu\text{m}$ excess emission is very weak and dependent on the correction for interstellar extinction.

UV Cas shows a large flux variation between IRAS and Spitzer observations. The IRAS $12 \mu\text{m}$ and $25 \mu\text{m}$ fluxes are factors of 6 (the highest value for our sample) and 3 (the second highest value for our sample), respectively, greater than the Spitzer values. A fit to the IRAS fluxes and ground-based photometry requires a blackbody at about 800 K and a higher R ($=0.28$) than required by the Spitzer fluxes (Figure 6 – righthand panel).

Bogdanov et al.’s (2010) survey shows that at the time of the IRAS observations UV Cas was unusually bright in the infrared. The L magnitude was almost two magnitudes brighter than when the star was observed by Spitzer and 0.8 magnitudes brighter than the 1973 measurement reported by Rao (1980). The M magnitude was about 1.5 magnitudes

brighter than in 2008. This IR excess observed by IRAS decayed over about 2000 days and was followed much later by two minor increases by about 0.6 magnitudes in L for a duration of about 1000 days without a pronounced optical decline. Evidently, UV Cas is an irregular infrared variable without contemporary optical variability. Bogdanov et al.’s L and M magnitudes are quite well reproduced by the fit to the IRAS fluxes (Figure 6 – righthand panel).

S Aps: S Aps is a cool RCB with a slightly less than average tendency to go into decline; Jurcsik (1996) gives the inter-fade period as 1400 days.

The UBVR_IJHKLMN magnitudes were assembled from the following sources: UB_V (Zhilyaev et al. 1978), UB_VR_I (Marang et al. 1990), JHK_L (Table 2), MN (Kilkenny & Whittet 1984). The adopted reddening is $E(B-V) = 0.05$ (Asplund et al. 1997). Feast et al. (1997) estimated $E(B-V) = 0.13$ but at such low reddenings the correction to the Spitzer and IRAS fluxes is unimportant.

A blackbody fit to the dereddened optical photometry gives a stellar temperature of 4200 K. De-reddened Spitzer fluxes and the contemporaneous JHK_L photometry are well fit with the stellar 4200 K and a dust blackbody at 750 K with dust dominating the star at wavelengths at K and beyond. The covering factor $R = 0.37$ is a typical value.

S Aps is a striking example where not only are the IRAS and Spitzer fluxes very similar but where measures of the IR excess at other times indicate an almost invariant excess and suggest a circumstellar environment containing a large number of dust clouds. For example, earlier photometry at KL (Glass 1978; Feast et al. 1997) and MN (Kilkenny & Whittet 1984) are reproduced satisfactorily by the stellar-dust blackbody combination. Variations of no more than several tenths of a magnitude at L are indicative of only minor variations in the cloud population in the circumstellar environment.

SV Sge: SV Sge is a cool RCB experiencing declines at a typical rate; Jurcsik (1996) gives the inter-fade period as 2500 days. Spitzer observed the star at maximum (Table 2).

The UBVR_I magnitudes for maximum light are taken as follows: VRI (Table 2), JHK (2MASS) and a B magnitude by assuming a (B-V) identical to that of the HdC star HD 137613 because the HdC and SV Sge have similar K-band spectra (García-Hernández et al. 2010). A reddening $E(B-V) = 0.72$ is adopted; a larger reddening results in an emission bump at $9.7 \mu\text{m}$, a feature shown by no other RCB.

The SED is well fit with a stellar blackbody of 4200 K and dust blackbodies of 565 K and 350 K which in total correspond to a covering fraction $R = 0.074$. The IRAS 25 μm flux agrees well with the Spitzer flux but the 12 μm flux is almost double the Spitzer

value which demands a hotter blackbody (720 K), a larger covering factor $R = 0.15$ with the same stellar blackbody. This flux increase at the time of the IRAS measurement implies a rather fresh ejection of dust. Perhaps, this ejection was responsible for the three magnitude optical decline which began in 1981 January and ended 1982 November. The dust emission contributes a few per cent of the K flux at the time of the Spitzer observation but approaches 10 per cent at the time of the IRAS observations.

Z UMi: This cool star identified as a RCB by Benson et al. (1994) is frequently in decline; since the star was put on the AAVSO program, it has shown nine declines in 16 years. Kipper & Klochkova’s (2006) analysis led them to suggest Z UMi is a minority RCB of low metallicity with a lithium excess (Goswami et al. 1997). Jurcsik (1996) did not include Z UMi in her determination of inter-fade periods. Spitzer observations were obtained as Z UMi was about two magnitudes below maximum light and recovering from the deepest longest lasting decline on record. The star is at a Galactic latitude of 33° and, therefore, we assume negligible interstellar reddening.

The stellar blackbody temperature is taken as 5200 K, a value consistent with the spectroscopic estimate of 5250 ± 150 K (Kipper & Klochkova 2006). Photometry for BVI from AAVSO and JHK from 2MASS at maximum light is fitted by this blackbody. A fit to the Spitzer spectrum calls for a blackbody at 710 K and a covering factor $R = 0.43$. Since the optical depth of the cloud(s) along the line of sight likely varies with wavelength, the adopted fit underestimates the (small) stellar contribution at infrared wavelengths.

The IRAS fluxes about 60% greater than Spitzer values suggest a blackbody at 850 K and a covering factor $R = 0.95$, a value higher than from the Spitzer fluxes at a time when the star was below maximum light.

V1783 Sgr: At the time of the Spitzer observation, V1783 Sgr was near maximum light following the deepest decline in 20 years, a decline that began about 2002 October and ended with restoration to maximum light about 2007 July. Apart from this unusually long but not particularly deep (about three magnitudes) decline, V1783 Sgr has shown only three declines over two decades.

Photometry obtained almost simultaneously with the Spitzer observations is in Table 2. Extensive UBVR photometry at maximum light was reported by Lloyd Evans et al. (1991) who proposed V1783 Sgr as a cool RCB. The VRI magnitudes in Table 2 are within the range reported by Lloyd Evans et al. An interstellar $E(B-V) = 0.42$ is suggested by the elimination of the absorptions at $9.7 \mu\text{m}$ and $18 \mu\text{m}$ from the Spitzer spectrum.

By combining Lloyd Evans et al.’s photometry with the JHK photometry from Table 2 and correcting for the interstellar reddening, the SED is fit with a stellar blackbody tem-

perature of 5600 K and dust blackbody of 560 K for a covering factor of $R = 0.28$. The color-corrected IRAS 12 μm and 25 μm fluxes are similar to the Spitzer values, giving a slightly hotter dust blackbody of 600 K with a covering factor of $R = 0.30$.

The 2MASS JHK are about a magnitude brighter than values in Table 2, and since the star was at visual maximum at the time of the 2MASS observation, it would appear that warm dust was present but off the line of sight.

WX CrA: This cool RCB observed by Spitzer at maximum light experiences declines at a typical frequency; Jurcsik (1996) gives the inter-fade period as 2000 days. Maximum light UBVR photometry was taken from Marang et al. 1990). The 2MASS JHK photometry agrees well with earlier measurements by Feast et al. (1997). Feast et al’s L magnitude and Kilkenny & Whittet’s (1984) M and N magnitude complete the available photometry at maximum light. Interstellar reddening is slight: $E(B-V) = 0.06$ (Rao 1995 in Asplund et al. 1997; Feast et al. 1997)

A fit to the maximum light reddening-corrected photometry and the Spitzer spectrum calls for a stellar blackbody at 4200 K and dust at 575 K and 120 K with covering factors of $R = 0.15$ and 0.006, respectively.

WX CrA is one of the few stars in the sample with IRAS fluxes, especially at 12 μm , that are much greater than Spitzer values. The IRAS fluxes require a blackbody at 700 K with a $R = 0.49$. This also accounts for the L and N magnitudes but not the M magnitude from Kilkenny & Whittet (1984). Glass’s (1978) M magnitude is 0.8 magnitudes fainter and falls close to the fit to the IRAS fluxes. Glass comments: ‘Long-term variations, not closely associated with visible-region behaviour, were observed at L.’ By extension, we infer these variations occur at longer wavelengths too.

V3795 Sgr: This star observed by Spitzer at maximum light is a warm ‘minority’ RCB which has undergone only two declines in the last 20 years with each lasting about five years; Jurcsik (1996) gives the inter-fade period as 6000 days, one of the longest in her sample.

VRI and JHK photometry (Table 2) was obtained almost simultaneously with the Spitzer observations. A B magnitude is estimated by combining the V from Table 2 with the (B-V) from Kilkenny et al. (1985). JHK magnitudes from Table 2 and 2MASS are in fair agreement. There are slight differences between these values and those provided by Feast et al. (1997) who also gave a N magnitude. Asplund et al. 1997 estimates $E(B-V) = 0.79$ but Feast et al. adopted $E(B-V) = 0.45$; here, the higher value is assumed.

The stellar blackbody temperature is set at 8000 K, the effective temperature estimated from spectroscopy by Asplund et al. (2000). A dust temperature of 610 K and a covering

factor $R = 0.31$ fit the dereddened Spitzer fluxes. The IRAS $12\ \mu\text{m}$ and $25\ \mu\text{m}$ fluxes, which are only slightly greater than Spitzer values, require a dust blackbody of 720 K and a covering factor $R = 0.54$. This accounts quite well for the flux at L from Feast et al. (1997) obtained when the star was at maximum. Feast et al.’s K magnitude is 0.5 magnitude brighter than the 2MASS and Table 2 values suggesting that warm dust affected their measurement at K.

V1157 Sgr: This cool RCB (Lloyd Evans et al. 1991) has undergone at least three minima in the last 20 years. According to the more recent ASAS-3 database, V1157 Sgr has experienced at least five minima of more than 2 magnitudes in the last nine years. When Spitzer observed the star it was about two magnitudes below maximum light (Table 2).

Available photometry is limited to that in Table 2 and the 2MASS JHK results. Adopting the latter as a measure of the star at maximum light and with an $E(B-V)$ of 0.3 estimated from a comparison of colors with those of HdC stars, a fit suggests a stellar blackbody temperature 4200 K and dust blackbodies at 770 K and 120 K with covering factors of $R = 0.59$ and 0.007, respectively. The 2MASS K magnitude received approximately equal contributions from the star and the dust. The IRAS $12\ \mu\text{m}$ and $25\ \mu\text{m}$ fluxes, which are greater than the Spitzer fluxes require dust at 850 K.

Y Mus: Y Mus, a warm RCB, has not experienced a decline in more than 20 years. Jurcsik (1996) gives the inter-fade period as 15300 days, the third longest in her list. Feast et al. (1997) note a brief decline in 1953 reported by Siedel (1957).

Simultaneous ground-based photometry was not obtained but in light of the star’s insistence on remaining at maximum light, photometry in the literature may be used to construct the SED. UBVRI photometry is taken from Kilkenny et al. (1985). JHK 2MASS measurements agree with a single observation by Feast et al. (1997) who also provide an L magnitude. Kilkenny & Whittet (1984) give M and N from 1983, the IRAS epoch. An interstellar $E(B-V) = 0.5$ is adopted (Feast et al. 1997; Asplund et al. 1997).

Reddening corrected fluxes are well fit by a stellar blackbody at 7200 K and a dust blackbody at 395 K with the low covering factor $R = 0.01$ (Figure 7).

Strikingly, the infrared excess from IRAS fluxes are considerably stronger: IRAS $12\ \mu\text{m}$ and $25\ \mu\text{m}$ fluxes are 4.5 and 2.9 times the Spitzer values, respectively. The 1983 MN observations (Kilkenny & Whittet 1984) span the IRAS fit: M is about 50% stronger and N is about 20% weaker than the IRAS fit. L (Feast et al. 1997) is matched by this fit to the IRAS fluxes. Only RT Nor and UV Cas have comparable ratios of IRAS to Spitzer fluxes. The fit to the IRAS fluxes and UBVRIJHKMN photometry gives a dust temperature of 590 K with a covering factor $R = 0.07$.

Evidently, this infrequently declining RCB had an unusually weak circumstellar dust shell at the time of the Spitzer and IRAS observations.

V739 Sgr: This is a cool RCB discovered by Lloyd Evans et al. (1991). The V magnitude (Table 2) agrees very well with the value listed in the ASAS-3 database indicating that the star was at maximum light at the time of the Spitzer observations. Sparse AAVSO measurements of the visual magnitude across 20 years suggest the star may be a frequent decliner. This is corroborated by the ASAS-3 database, which shows at least four declines in the last nine years.

Photometry is available at VRIJHK from Table 2. The interstellar reddening is assumed to be $E(B-V)=0.5$, the estimate for VZ Sgr in the same direction. A fit to the dereddened photometry and Spitzer fluxes gives a stellar blackbody of 5400 K with the K-band dominated by the dust emission. Spitzer fluxes are well fit with a 640 K blackbody with a covering factor $R = 0.59$ and there is a hint of a cooler blackbody at 100 K with $R \simeq 0.005$. The K flux which is not primarily from the star suggests the presence of dust hotter than 640 K. The IRAS 12 μm flux is within a few per cent of the Spitzer flux. This close correspondence and the fact that the 25 μm IRAS flux is of low quality makes the fit to the IRAS fluxes more uncertain. Two blackbodies of 900 K and 700 K with $R = 0.64$ and 0.228, respectively, can fit the K band flux and the IRAS photometry simultaneously.

VZ Sgr: This warm ‘minority’ RCB has experienced several declines of differing depths in the last 20 years; Jurcsik (1996) gives the inter-fade period as 1300 days. At the time of the Spitzer observations, VZ Sgr was recovering from a deep prolonged decline and still several magnitudes below maximum.

Stellar fluxes for the star at maximum light are taken from the literature: UBVRJ (Kilkenny et al. 1985), JHK (Feast et al. 1997; 2MASS), and L (Feast et al. 1997). The interstellar reddening is $E(B-V)=0.30$ (Feast et al. 1997).

The fit to the dereddened photometry and Spitzer fluxes gives a stellar blackbody at the spectroscopic effective temperature of 7000 K (Asplund et al. 2000) and dust at temperatures of 700 K and 140 K with covering factors of $R = 0.17$ and 0.008, respectively (Figure 8). The IRAS 12 μm and 25 μm straddle the Spitzer fluxes. Additionally, the L magnitude from June 1995 (Feast et al. 1997) is well matched by the dust’s contribution at 700 K with a small contribution from the star. The K magnitude is slightly contaminated by dust emission. These data suggest that the dusty envelope has maintained a high degree of uniformity over decades.

U Aqr: U Aqr, a cool RCB in the Galactic halo, is distinguished by its extraordinary enrichment of light *s*-process (e.g., Sr) nuclides but a near-normal abundance of heavy *s*-

process (e.g., Ba) nuclides (Bond et al. 1979; Vanture et al. 1999). Jurcsik (1996) puts the inter-fade period at 1850 days but in the last 20 years, U Aqr has spent about 10 years below maximum light. When the Spitzer observations were obtained, U Aqr was about 0.6 magnitudes in V below maximum light in a slow recovery from a deep decline.⁵

The SED is constructed from photometry acquired at maximum light. The interstellar reddening for this halo star about 10 kpc above the Galactic plane (Lawson & Cottrell 1997) is slight: $E(B-V)=0.05$ (Rao 1995 in Asplund et al. 1997; Feast et al. 1997). Photometry is from the following sources: UBVRI (Lawson et al. 1990; Marang et al. 1990), JHK (2MASS), JHKL (Feast et al. 1997).

The blackbody combination of 5000 K for the star and 475 K and 140 K for the dust fits the data with covering factors of 0.23 and 0.021 for the cool blackbodies.

The IRAS fluxes straddle the Spitzer spectrum: the IRAS flux at 12 μm exceeds its Spitzer counterpart but the IRAS upper limit at 25 μm is less than the Spitzer value. A fit to the IRAS data suggests a dust blackbody at 560 K with a covering factor of 0.37. This warmer black body fits the L magnitude from Feast et al. (1997).

MACHOJ181933: This is a cool RCB discovered by Zaniewski et al. (2005). Comparison of photometry in Table 2 and from the discovery paper show that the star was at maximum light at the time of the Spitzer observations. Nothing is yet known about the frequency of declines.

VRI (Table 2) and JHK (2MASS) photometry are available. The interstellar reddening is uncertain but not negligible; the star is in the direction of the Galactic Bulge. Zaniewski et al. (2005) put $E(B-V)$ at 1.0. Here, we adopt $E(B-V)=0.5$.

A fit to VRIJHK fluxes and the Spitzer spectrum is obtained with a stellar blackbody of 4200 K and blackbodies of 695 K and 140 K with covering factors of 0.48 and 0.022, respectively, for the latter two blackbodies. The stellar temperature is similar to that of S Aps.

ES Aql: ES Aql, a cool RCB (Clayton et al. 2002) declines quite frequently: AAVSO and ASAS-3 observations show a major decline about every year. Not surprisingly, Spitzer caught ES Aql recovering from a deep decline; it was at $V=12.3$ or about 0.8 magnitudes below maximum light. There is no multicolor photometry for ES Aql at maximum light.

⁵High-resolution spectra in sample regions of the K band obtained less than two months before the Spitzer observations show stellar molecular absorption features and, therefore, the star not the dust was the dominant contributor to the K band (García-Hernández et al. 2010).

BVRI at maximum are inferred from Clayton et al.’s Table 1 and discussion. JHKL magnitudes⁶ are also from Clayton et al. (2002). Adopting an interstellar reddening $E(B-V)=0.32$ (Clayton et al. 2002) and a stellar blackbody of 4500 K fitted to the dereddened BVRI, the Spitzer fluxes are fit with a 700 K blackbody and a covering factor of 0.49 (Figure 9). The L magnitude from 1997 June fits the SED composed of the 4500 K and 700 K blackbodies which is expected because for active stars like ES Aql the L magnitude is little affected as a star goes from maximum to minimum. IRAS 12 μm and 25 μm fluxes are within 10% of their Spitzer values.

FH Sct: This warm RCB has been largely ignored by observers probably because it appears within (but beyond) the Galactic cluster NGC 6694 (M 26). At the time of the Spitzer observations, FH Sct was at 13.00 (Table 2) in agreement with the ASAS-3 database and suggesting that it was about 0.5 magnitudes below maximum.

VRI are taken from Table 2. 2MASS JHK are assumed to refer to maximum light. A reddening $E(B-V)=1.0$ is adopted from a comparison of (B-V) colors of FH Sct with RCBs of similar temperature.

A stellar blackbody of 6250 K (the spectroscopic effective temperature - Asplund et al. 2000) is adopted and the Spitzer spectrum is fitted by blackbodies of 540 K and 140 K with covering factors $R = 0.10$ and $R = 0.002$, respectively. FH Sct is a rare case where the IRAS 12 μm flux is less than the Spitzer flux. The IRAS 25 μm flux of moderate quality is similar to the Spitzer value.

SU Tau: This warm RCB frequently experiences declines; SU Tau has been three or more magnitudes below maximum light for nearly half of the last 20 years. Jurcsik (1996) gives the inter-fade period as 1200 days. Despite its propensity to live below maximum light, the photometry reported in Table 2 shows that it was at maximum light during the Spitzer observations.

The SED was constructed from the following: UBV (Ferne et al. 1972), VRI (Table 2), and JHKL (Table 2). The 2MASS JHK are 1.4, 1.0, and 0.4 magnitudes, respectively, fainter than those in Table 2 but were measured when SU Tau was recovering from a deep decline. Interstellar reddening of $E(B-V)=0.50$ (Glass 1978; Feast et al. 1997) is adopted.

Adopting a stellar blackbody at 6500 K, the spectroscopic effective temperature (Asplund et al. 2000), the Spitzer spectrum and the L flux are matched with a 635 K blackbody with a covering factor $R=0.45$. A fit to the UBVRIJHK fluxes gives a stellar blackbody

⁶Note that the 2MASS magnitudes of ES Aql are not saturated as stated by Clayton et al. (2002) (Clayton 2011, private communication).

temperature of 6500 K, the spectroscopic effective temperature (Asplund et al. 2000). IRAS 12 μm and 25 μm fluxes are both slightly higher than Spitzer fluxes.

DY Per: This RCB advertised to be ‘the coolest metal-poor’ RCB (Yakovina et al. 2009) declines at approximately two year intervals. At the time of the Spitzer observations, DY Per was at $V \simeq 11.8$ or about 0.5 magnitudes below maximum light and at the beginning of a decline that eventually reached a depth of more than five magnitudes below maximum light. Yet it is not very clear if DY Per-like stars really are RCB stars (e.g., Alcock et al. 2001).

We assemble published VBRIJHKLM magnitudes made at or near maximum light (Začs et al. 2007; Alksnis et al. 2009) and adopt the reddening $E(B-V)=0.48$ (Začs et al. 2007). The 2MASS JHK magnitudes are about 0.4 magnitudes fainter than the adopted values, an indication that they were obtained during a decline.⁷

A fit to the dereddened photometry and the Spitzer spectrum with a stellar blackbody at 3000 K (Yakovina et al. 2009) requires blackbody at 1400 K for the dust. The IRAS fluxes are so similar to Spitzer values that a separate fit was not made. With this combination, JHKL are dominated by the dust contribution. The stellar temperature is somewhat hotter than Yakovina et al.’s (2009) estimate of 2900-3100 K from model atmosphere predictions fitted to a 4300-7300 Å SED but this apparent discrepancy may be due to the presence of strong molecular absorption bands which are not taken into account by a blackbody representation of a SED. More significantly, Tenenbaum et al. (2005) show that the first- and second-overtone CO bands are seen in the K and H bands, respectively, showing that the star dominates the flux in these bands. The M-band flux is well below that implied by the 1700 K blackbody and may be due to strong CO fundamental band absorption. The IRAS and Spitzer fluxes are very similar.

The Spitzer spectrum has a short wavelength cutoff at 10 μm and, therefore, no information is provided about the 6-10 μm feature widely seen in RCB spectra. However, DY Per’s spectrum shows a sharp emission feature at 11.3 μm on a ‘pedestal’ extending from about 10 μm to 13.5 μm .

V517 Oph: Kilkenny et al. (1992) identified V517 Oph as cool RCB which is ‘very active in the RCB sense’, i.e., frequently in decline. This is corroborated by more recent ASAS-3 measurements, which show several minima in the last nine years. The optical spectrum shown by Kilkenny et al. shows great similarity with S Aps. At the time of

⁷Záčs et al. report that DY Per has a visual companion, a G0 dwarf at a separation of 2.5 arc sec. This is unlikely to contribute to the SED.

the Spitzer observations, the star at $V=14.05$ (Table 2) was about 2.4 magnitudes below maximum light.

Photometry in Table 2 enables the stellar SED to be estimated as it was at the time of the Spitzer observations but it is more valuable for understanding the relation between dust and star to analyse the SED at maximum light. Unfortunately because the star is faint and frequently in decline, measurements at maximum are rare. UBVI photometry reported by Kilkenny et al. was, as they noted, obtained below maximum light: their brightest $V=12.4$ may be about one magnitude fainter than maximum light values from the AAVSO and ASAS-3 databases. 2MASS JHK magnitudes are 2.2 (J), 1.5(H), and 0.8 (K) magnitudes brighter than those in Table 2. Kilkenny et al. estimate $E(B-V)=0.5-0.6$.

A fit to the 2MASS photometry is possible with a stellar blackbody of 4100 K and a dust blackbody of 850 K with a covering factor of 0.84. This fit accounts quite well for the L flux (Table 2) and a substantial amount of the flux at K is from the dust. The IRAS fluxes are somewhat larger than Spitzer values: 20% at $12\ \mu\text{m}$ and 10% at $25\ \mu\text{m}$ over Spitzer values.

V CrA: This warm minority RCB was observed by Spitzer at maximum light following a deep decline two and a half years previously. The star frequently declines; Jurcsik (1996) gives the inter-fade period as 900 days and only three stars in her sample decline more often.

Photometry at maximum light is taken from the literature: UBVI (Lawson et al. 1990) and JHK (Feast et al. 1997; Glass 1978). 2MASS JHK measurements are fainter by 0.2 (J), 0.5 (H) and 0.7 (K) magnitudes than Feast et al.’s mean values. Kilkenny & Whittet (1984) measured the M and N magnitudes at a time when the star was at least three magnitudes below its maximum visual brightness. V CrA is only slightly reddened: $E(B-V) = 0.14$ (Rao 1995 in Asplund et al. 1997).

A fit to the UBVI fluxes and the Spitzer fluxes with a 6500 K stellar blackbody, the spectroscopic effective temperature (Rao & Lambert 2008), calls for dust blackbodies at 550 K and 150 K with covering factors of 0.38 and 0.020, respectively. This fit does not account for the 2MASS HK and the above LMN magnitudes, all of which are consistently brighter than the Spitzer spectrum. Clearly, the infrared flux varies considerably. The IRAS $25\ \mu$ flux and the KLMN fluxes, all observed at different times, are reasonably well fit with a 6500 K blackbody and dust at 1600 K, 900 K, and 550 K with covering factors of $R = 0.23, 0.37,$ and $0.37,$ respectively. However, the IRAS $12\ \mu\text{m}$ flux is about $\sim 15\%$ larger than suggested by our blackbody fitting. This suggests that the dust may be distributed in a disk rather than in a simple discrete cloud or shell. Indeed, Bright et al. (2011) report possible asymmetries in the V CrA’s circumstellar dust shell from VLTI interferometric data at $10\ \mu\text{m}$.

RZ Nor: RZ Nor is a warm RCB notable for the presence of lithium. Jurcsik (1996) gives the inter-fade period as 1100 days, a typical value. According to the ASAS-3 database, the Spitzer observations were obtained when RZ Nor was at maximum light.

Photometry at maximum light is provided by Glass (1978) for JHKL, Kilkenny et al. (1985) for UBVRI and by Feast et al. (1997) for JHKL. Kilkenny & Whittet (1984) observed at M and N when the star was about two magnitudes below maximum. Also, the 2MASS observations were obtained at a minimum when J was 3.8 and K was 0.9 magnitudes fainter than Feast et al.'s estimates for maximum light. A reddening of $E(B-V)=0.5$ is adopted (Glass 1978; Kilkenny & Whittet 1984; Rao 1995 – see Asplund et al. 1997; Feast et al. 1997).

Fluxes from U to H are fit by a stellar blackbody of 5000 K, a temperature lower than the spectroscopic effective temperature (Asplund et al. 2000). Spitzer fluxes are fit with blackbodies of 700 K and 320 K with a hint of a 25 K blackbody introduced to account for a flux increase longward of $34 \mu\text{m}$. The covering factors are 0.53 and 0.035 for the 700 K and 320 K blackbodies, respectively. IRAS fluxes for $12 \mu\text{m}$ and $25 \mu\text{m}$ can be fit with a similar combination of blackbodies at 700 K and 300 K and covering factors of 0.53 and 0.040, respectively.

RT Nor: RT Nor, a warm RCB, was at maximum light when observed by Spitzer. Its last decline occurred about 15 years before. This fact demonstrates the statistical nature of RCB declines because Jurcsik (1996) gives the inter-fade period as short as 1950 days.

Photometry of RT Nor at maximum light is assembled from the literature: UBVRI (Kilkenny et al. 1985), JHKLM Glass (1978), JHK (2MASS), JHKL (Feast & Glass 1973), MN (Kilkenny & Whittet 1984). Although limited in coverage, the photometry at LMN suggests strong variability. For example, Feast et al. (1973) give $L=6.42$ whereas Glass (1978) reports a range from 7.6 to 8.3 from five observations. Similarly, Kilkenny & Whittet (1984) give $M=5.8$ but Glass measured $M=4.8$. Interstellar reddening of $E(B-V)=0.39$ (Glass 1978; Kilkenny & Whittet 1984; Rao 1995) is assumed.

A stellar blackbody of 6700 K and dust blackbodies of 320 K and 130 K with remarkably low covering factors of 0.01 and 0.001, respectively, provide a satisfactory fit to the UBVRIJK and Spitzer fluxes (Figure 10 - lefthand panel). It is not surprising that the excess emission at $6\text{--}10 \mu\text{m}$ is also unusually weak for RT Nor.

Dust emission was much stronger at the time of the IRAS observations. The ratio IRAS to Spitzer fluxes is a factor of five at $12 \mu\text{m}$ and three at $25 \mu\text{m}$. A fit to the IRAS fluxes requires a blackbody of 500 K and a covering factor of 0.11 (Figure 10 – righthand panel). This fit does not account for the LMN fluxes: the LM fluxes are greater than the 500 K

blackbody but at N the flux is less than that blackbody. A fit solely to the UBVR_IJHKLMN fluxes calls for the stellar blackbody to be accompanied by a dust blackbody of 920 K with a covering factor of 0.11. The limited observational data suggests that RT Nor experienced a increase in its infrared excess around 1980.

RS Tel: RS Tel, a cool RCB, was observed by Spitzer shortly before it underwent a prolonged decline. This decline apart, RS Tel has experienced no major declines and only one minor decline of about two and a half visual magnitudes in the last two decades. However, Jurcsik (1996) gives the inter-fade period as 1200 days.

Photometry at maximum light is taken from the literature: UBVR_I (Kilkenny et al. 1985; JHKLM (Glass 1978), Goldsmith et al. 1990), JHK (2MASS), JHKL (Feast et al. 1997) and MN (Kilkenny & Whittet 1984). The interstellar reddening is taken to be $E(B-V) = 0.17$ (Feast et al. 1997; Kilkenny & Whittet 1984; Rao 1995 – see Asplund et al. 2000; Bergeat et al. 1999).

Optical and Spitzer fluxes are well fit by a stellar blackbody of 6750 K, the spectroscopic effective temperature, and blackbodies of 720 K and 130 K with covering factor of 0.25 and 0.005, respectively (Figure 11).

The IRAS 12 μm and 25 μm fluxes are just 10% greater than Spitzer values, suggesting a slightly cooler dust blackbody of 620 K and a covering factor of 0.22. Also, the LMN fluxes are quite well reproduced by the combination of the 6750 K and 720 K blackbodies. Since the LMN and IRAS photometry were obtained decades prior to the Spitzer spectrum, the ability of a single fit to match all the observations implies long-term uniformity of the circumstellar envelope.

V482 Cyg: The RCB V482 Cyg has a K5III companion only 6 arc sec away (Gaustad et al. 1988; Rao & Lambert 1993). The star was at maximum light when observed by Spitzer. It has experienced just two declines in 20 years, one 14 and the other 19 years ago. Jurcsik (1996) gives the inter-fade period as 3400 days.

Photometry at maximum light is assembled from the literature: BVRI (Rosenbush 1995), JHK (2MASS), JHKL (Gaustad et al. 1988). An interstellar reddening of $E(B-V) = 0.5$ is adopted (Rao & Lambert 1993).

The BVRIJHK fluxes are well fit with a blackbody of 4800 K which with blackbodies at 500 K and 100 K with covering factors of 0.03 and 0.001, respectively, combine to fit the Spitzer fluxes. The stellar blackbody is considerably cooler than the 6750 K effective temperature provided by Asplund et al. (2000) from their abundance analysis.

The IRAS 12 μm and 25 μm fluxes are 80% and 10%, respectively, greater than Spitzer

fluxes. A fit to the BVRIJHK and IRAS fluxes with the 4800 K stellar blackbody demands a 650 K blackbody and a covering factor of 0.09. Neither the IRAS nor the Spitzer fit accounts for the flux at L measured in 1984. This requires a blackbody of about 1800 K, a temperature hotter than the sublimation temperature of carbon soot, which may result from contamination by the K5 companion.

MV Sgr: This hot RCB star, according to De Marco et al. (2002), falls outside the reach of ‘current stellar evolutionary models’, i.e., the star is not readily attributable to either the FF or DD scenarios. MV Sgr rarely experiences a decline; the last recorded decline was in the 1950s (Hoffleit 1959). Thus not surprisingly, Spitzer observed the star at maximum light.

Photometry is taken from the following sources: UBVR (Kilkenny et al. 1985; Goldsmith et al. 1990), JHKLMN (Kilkenny & Whittet 1984) and JHK (2MASS). DeMarco et al. estimate $E(B-V)=0.43$.

De-reddened BVRI fluxes are well fit with a blackbody of temperature 15400 K, the effective temperature estimated from spectroscopy by Jeffery et al. (1988) but other temperatures will fit these fluxes in the Rayleigh-Jeans tail. The Spitzer spectrum is matched with blackbody at 205 K and a covering factor of 0.18. The IRAS fluxes are reproduced by a slightly hotter 235 K blackbody with a slightly larger covering factor. This increase also fits the N flux but the M flux exceeds the fit by a factor of about 50 per cent.

The limited photometry at JHKLMN indicates the presence of a variable source with a temperature of 1500K or so. For example, the JHKL fluxes require in addition to the 15400 K and 205 K blackbodies a blackbody at 1500 K with a covering factor of 0.33. A fit to IRAS and MN fluxes requires 1500 K and 235 K blackbodies together with the stellar 15400 K blackbody to fit BVRI. This combination predicts too strong a flux at K. This contribution at about 1500 K may come from fresh production of carbon soot.

RY Sgr: For RY Sgr, a warm RCB, deep declines occur about every 4 years and the Spitzer observations were made when RY Sgr was about three magnitudes below maximum light. Jurcsik (1996) gives the inter-fade period as 1400 days.

The star is represented by a 7200 K blackbody; the spectroscopic effective temperature is 7250 K (Asplund et al. 2000). The Spitzer fluxes are fit with a blackbody of 675 K and a covering factor of 0.20.

Fluxes measured by ISO from 4 μm to 26 μm exceed Spitzer values and suggest a dust blackbody of 820 K with a covering factor of 0.38. IRAS fluxes which exceed both ISO and Spitzer values are fit with a dust blackbody of 870 K and a covering factor of 0.76. It

is tempting in the sequence of declining blackbody temperatures and covering factors from IRAS to ISO to Spitzer to see an evolutionary sequence from IRAS in 1983 to ISO in 1997 and then to Spitzer in 2004 October. In light of the frequency of declines, an evolutionary interpretation is probably too simplistic. Bright et al. (2011) report the apparent presence of asymmetric circumstellar material around RY Sgr.

V854 Cen: V854 Cen, a most active warm RCB, has the shortest known inter-fade period (370 days) of the RCBs studied by Jurcsik (1996). Spitzer observations were obtained when V854 Cen was at a visual magnitude between five and six magnitudes below maximum. An important distinguishing mark is its modest H-deficiency among RCBs: hydrogen is deficient by a factor of only 100 to 1000 (Asplund et al. 1998).

Published photometry for maximum light is available from Lawson et al. (1999) for UBVRI and Feast et al. (1997) for JHKL. Interstellar reddening $E(B-V)=0.07$ is adopted (Feast et al. 1997).

BVRI are quite well fit with a blackbody of 6750 K, the spectroscopic effective temperature (Asplund et al. 1998). The Spitzer spectrum is fit by a blackbody combination of 900 K and 140 K with covering factors of 0.32 and 0.03, respectively. This fit accounts fairly well for the HKL at minimum light, the phase at which V854 Cen was when observed by Spitzer.

IRAS fluxes are stronger than Spitzer values and similar to the ISO values (Lambert et al. 2001). The fit to IRAS (and ISO) fluxes requires a 1100 K blackbody with a covering factor of unity. The HKL fluxes at optical maximum are dominated by dust emission; the flux increases with increasing wavelength. This fit accounts quite well for the JHKL fluxes at maximum light. Indeed, the ISO observation was made when V854 Cen was only slightly below maximum light. Very recent high angular resolution interferometric observations of V854 Cen show the possible presence of asymmetries in the circumstellar envelope (Bright et al. 2011).

UW Cen: UW Cen, a warm RCB, has an inter-fade period of 1100 days (Jurcsik 1996). A reflection nebula illuminated by the star was discovered by Polacco et al. (1991) and further studied by Clayton et al. (1999). Spitzer observations were obtained at maximum light during an approximately 18 month restoration to maximum light between an earlier deep decline lasting almost a decade and the next decline which ended early in 2010.

Photometry for maximum light is taken from the literature: UBVRI (Kilkenny et al. 1985; Goldsmith et al. 1990), JHKLM (Glass 1978), JHKL (Feast et al. 1997; Goldsmith et al. 1990), MN (Kilkenny & Whittet 1984; Goldsmith et al. 1990). Interstellar reddening $E(B-V)=0.32$ is assumed (Glass 1978; Kilkenny & Whittet 1984; Rao 1995 – see Asplund et al. 1997; Feast et al. 1997).

A fit to the dereddened fluxes with a 7500 K stellar blackbody, the spectroscopic effective temperature (Asplund et al. 2000), calls for blackbodies at 630 K, 120 K and 50 K with covering factors of 0.44, 0.013, and 0.05, respectively. Dust emission extends to the K band; the K-flux is greater than that at H.⁸ The fit to the Spitzer fluxes accounts well for the L and M fluxes observed about 30 years earlier. The N flux is less than the Spitzer value by about 20%. The IRAS 12 μm flux is in good agreement with the Spitzer value but the 25 μm flux is about 30% higher than the Spitzer measurement.

DY Cen: DY Cen, a hot RCB, has not experienced a decline in 20 years, although the maximum V magnitude seems to have fallen by 0.7 magnitude in 45 years (DeMarco et al. 2002). Jurcsik (1996) gives the inter-fade period as 6400 days. Lambert & Rao (1994), on the basis of the abundance analysis by Jeffery & Heber (1993), considered DY Cen to be a minority RCB. DeMarco et al. note that DY Cen is likely to be related to be the other (cooler) RCBs. The star is unusually H-rich for a RCB: H/He = 0.1 by number (Jeffery & Heber 1993).

Photometry in the literature provides the following: UB V (Pollacco & Hill 1991), UB V RI (Kilkenny et al. 1985), JHK (2MASS), N (Kilkenny & Whittet (1984). Interstellar reddening $E(B-V)=0.47$ is adopted (Jeffery & Heber 1993; Rao et al. 1993).

A stellar blackbody of 19500 K, the effective temperature obtained by Jeffery & Heber from their spectroscopic analysis, is fitted to the reddening-corrected UB V RIJHK fluxes. Since these bandpasses are in the Rayleigh-Jeans tail of a hot blackbody, other fits are possible. The Spitzer fluxes show that the dust is predominantly cool with a blackbody of 272 K and a covering factor of 0.09. Emission features from a mixture of PAHs and C_{60} molecules are prominent (García-Hernández et al. 2011). IRAS fluxes are within about 10% of the Spitzer values.

R CrB: R CrB is the most studied warm RCB. It was at maximum when the Spitzer spectrum was obtained. Jurcsik (1996) gives the inter-fade period as 1100 days.

The UB V RIJ fluxes are fit with a 6750 K blackbody, the spectroscopic effective temperature (Asplund et al. 2000). The 10-20 μm Spitzer spectrum is fitted with a 950 K blackbody with a covering factor of 0.30. This fit also accounts well for the K and L fluxes where the shell makes the dominant contribution to the latter and the star to the former. The IRAS 12 μ and 25 μm fluxes are higher than Spitzer values. The ISO spectrum from 1998 January in fair agreement with the IRAS fluxes was fit with a combination of two

⁸The fact that dust dominates the spectrum in the K band is confirmed by K-band spectra obtained in 2007 February when UW Cen was at maximum light (García-Hernández et al. 2009).

blackbodies: 1390 K and 610 K (Lambert et al. 2001). Rao & Nandy (1986) fitted the IRAS observations with a black body at 680 K and Clayton et al. (1995) fitted an IRAS LRS spectrum with a blackbody at 650 K. R CrB is a variable (out of decline) in the infrared. There are variations of about one magnitude at K and of two magnitudes at L. Strecker (1975) and Feast et al. (1997) suggest that the L variations follow a period of about 1260 days. Thus, a fit of infrared - optical SED requires a variable infrared excess.

V348 Sgr: V348 Sgr is ‘the second most active RCB star (after V854 Cen)’ (De Marco et al. (2002); Jurcsik (1996) gives the inter-fade period as 560 days. V348 Sgr is a hot RCB with an effective temperature about 22000K (Jeffery 1995). De Marco et al. (2002) suggest with some reservations that V348 Sgr is a final-flash post-AGB star becoming once again the central star of a planetary nebula. Visible nebulosity is present (Pollacco et al. 1990) supporting the evolutionary interpretation. Spitzer observations were obtained when V348 Sgr was undergoing a minimum and are discussed in more detail in Clayton et al. (2011).

Photometry at maximum light is assembled as follows: BVRI (Heck et al. 1985), JHKLM (Glass 1978), JHK (2MASS). Observed fluxes are corrected for an interstellar reddening of $E(B-V)=0.45$ (Pollacco et al. 1990).

Adopting a stellar blackbody at 20000 K, the Spitzer spectrum is fit with a combination of 707 K and 100 K blackbodies with covering factors of 0.63 and 0.035, respectively. This fit accounts well for the JHKLM fluxes from the 1970s and the 2MASS JHK from 1998. Also, the IRAS fluxes only slightly exceed their Spitzer counterparts. Rao & Nandy’s (1986) fit to the IRAS 12, 25, 60, and 100 μm fluxes required warm dust (600 K) and cold dust (60-100 K), a mixture very similar to the present fit to the Spitzer observations obtained nearly 30 years later. This constancy of the infrared emission over decades is not surprising given that V348 Sgr is secondmost active RCB.

HV 2671: De Marco et al. (2002) note that HV 2671 in the LMC and V348 Sgr have almost identical optical spectra. The Spitzer spectra are, however, very different (Figure 5; see also Clayton et al. 2011 for more details). De Marco et al. provide JHK magnitudes and a reddening estimate $E(B-V)=0.15$. Soszyński et al. (2009) report V and I for maximum light. On the assumption that the stellar blackbody temperature is 20000 K, the same as for V348 Sgr, the fit to the JHK fluxes and the Spitzer spectrum calls for blackbodies at 590 K and 150 K with covering factors of 0.36 and 0.268, respectively. There is a hint for the presence of an additional and very cool 40 K dust component with a negligible covering factor. The dust distribution around HV 2671 differs substantially from that around V348 Sgr, a not surprising result.

4. Probing the cloudy circumstellar environment

Early investigations of the infrared emission from RCBs searched for variability of that emission. Among the earliest studies of infrared variability, Forrest et al.’s (1972) observations of R CrB through a six-magnitude visual decline showed that the infrared flux from $3.5 \mu\text{m}$ to $11 \mu\text{m}$ remained essentially unaffected by the decline. This result suggested that the dust cloud causing the decline represents a small addition to the warm circumstellar material already in place.

Long-term monitoring of the infrared excess of RCBs potentially offer particular insights into the structure and growth of clouds in the circumstellar environment. In this regard, Feast and colleagues at the South African Astronomical Observatory (SAAO) provided a valuable set of observations. For example, Feast et al. (1997) report JHKL photometry of 12 RCBs for timespans of up to 23 years. At JHK, the star generally dominated the observed flux but at L the infrared excess from dust is significant. Observations at L along with other evidence led to the proposal that dust is ejected into the circumstellar environment in the form of ‘random puffs’ (Feast 1979, 1986, 1996, 1997; Feast et al. 1997).

It is in the context of the ‘puff’ model that we explore below what may be deduced from the relation between the Spitzer and IRAS fluxes and the dependence of the covering factor R on the frequency of optical declines. These relations suggest that dust is ejected in puffs, often off the line of sight, and very likely in most cases the ejection occurs approximately isotropically off the star (i.e., at random directions).

4.1. Spitzer versus IRAS

A comparison of the Spitzer spectra with the IRAS $12 \mu\text{m}$ and $25 \mu\text{m}$ fluxes provides insight into the variability of the emission from circumstellar dust on a time scale of about 25 years. This is potentially valuable because 29 of our RCBs are in the IRAS catalog. In Figure 12, we present histograms of the ratios of the IRAS to Spitzer fluxes at $12 \mu\text{m}$ (left panel) and $25 \mu\text{m}$ (right panel).

With the exception of five outliers, the ratios at $12\mu\text{m}$ are less than two: the mean value is $r_{12} = 1.41 \pm 0.35$ from 22 stars. A correction has to be applied because the IRAS fluxes refer to a broad-band and assigned an effective wavelength of $25 \mu\text{m}$. The effective wavelength assumes the energy distribution has the form $f_\nu \propto \nu^{-1}$ or $f_\lambda \propto \lambda^{-1}$. Given that the Spitzer spectra are close approximations to a blackbody spectrum, one may estimate a color correction according to a recipe provided in the IRAS catalog (Beichman et al. 1988). This color correction reduces the IRAS catalog entries by about 16 per cent or the ratio r_{12}

is 1.18.

Setting aside the same five outliers, the ratio $r_{25} = 1.27 \pm 0.32$ from 21 stars: R CrB was not observed by Spitzer at 25 μm and the ratios for VZ Sgr and U Aqr are set at the value given by the upper limit to their IRAS 25 μm fluxes. After the color correction, this value of r_{25} is not sensibly different from unity.

For stars with extended infrared emission, the IRAS fluxes will be systematically larger than Spitzer values because of the larger IRAS aperture. The IRAS aperture was approximately two minutes of arc which is larger than the Spitzer aperture for the SH observations ($4.7'' \times 11.3''$) used at 12 μm and for the LH observations ($11.1'' \times 22.3''$) used at 25 μm . Perhaps, coincidentally the 25 μm Spitzer fluxes through the larger LH aperture are closer to their IRAS counterparts than the 12 μm fluxes through the SH aperture. As we have already mentioned in Section 2.2, all RCBs in our sample are point-like sources for Spitzer. IRAS and Spitzer fluxes agree very well when astronomical sources are point-like for Spitzer (e.g., García-Hernández et al. 2007; 2009). Indeed, R CrB itself which is known to be extended shows no important flux differences between IRAS and Spitzer (also V348 Sgr with a PN of $30''$, Clayton et al. 2011). Thus, the presence of the five outliers is not related to a possible extended emission in these sources⁹. Finally, note that possible extended diffuse background emission is usually due to much colder dust (see e.g., Cox et al. 2011), which emits at wavelengths longer than 25 μm (see e.g., the case of the hot RCBs V348 Sgr and HV 2671; Clayton et al. 2011).

The IRAS-Spitzer comparison has, thus, shown that the circumstellar dust emission for the great majority of the RCBs is unchanged over the last couple of decades. This is not a surprising result given the extensive L band photometric measurements on a fair sample of RCBs conducted at the SAAO over several years (Feast et al. 1997). Attention is necessarily drawn to the five outliers. Before discussing this quintet, we note the surprising result that these outliers all with high values of r_{12} and r_{25} ¹⁰ can not be matched with a similar number of outliers with remarkably low values of r_{12} and r_{25} . Three of the five have r_{12} of between five and six. A comparable outlier on the low- r side of the histogram would have a value of less than 0.2, but the sole RCB with r_{12} of less than unity is FH Sct with $r_{12}=0.7$. With respect r_{25} , the asymmetry is not quite so severe. The lowest r_{25} values are upper limits of 0.9 and 0.8 for VZ Sgr and U Aqr, respectively to be compared with the highest two values of 3.3 and 2.9 for Y Mus and UV Cas, respectively. Is this presence of outliers on the high r and the paucity of outliers on the low r side just a statistical fluke or a hint at a long-

⁹Note also that extended emission is not seen in the available Spitzer/IRAC images at 8 μm .

¹⁰The r_{25} for WX CrA is 1.8, a value which does not qualify it as an outlier at 25 μm .

term evolution in RCB dust shells? The latter seems unlikely given that the evolutionary timescale is likely to be a few thousand years and the interval between IRAS and Spitzer observations is less than 30 years.

With respect to the outliers, a possible explanation is that these are RCBs which rarely eject dust. Dust ejection rates may or may not be closely related to the frequency of declines, i.e., formation and presence of dust along the line of sight. Dust formation may or may not occur in preferential directions such as an equatorial plane or as polar plumes. Next, we discuss the five outliers in order of decreasing r_{12} : three – Y Mus, UV Cas, and RT Nor – have $r_{12} \simeq 5$ and two – WX CrA and RY Sgr – have $r_{12} \simeq 3$.

Y Mus: Y Mus has not experienced a decline in the nearly thirty years covered by AAVSO records which begin about 1982 January. The covering factor $R = 0.009$ from the Spitzer observations is the lowest among our RCB sample. Even the IRAS fluxes correspond to a low $R = 0.07$. Thus, we conclude that Y Mus is simply a poor producer of dust, i.e., the preferred axis for dust production is not orthogonal to the line of sight. One supposes that Y Mus is slightly more active with respect to dust production than XX Cam which has not been observed in decline at all and has no infrared excess out to $10 \mu\text{m}$ (Rao et al. 1980).

UV Cas: At the time of the IRAS observations, UV Cas was considered to be a typically dusty RCB with a covering factor $R = 0.28$ but by the time that Spitzer observed it the infrared fluxes had declined sharply and the covering factor had dropped to $R = 0.03$. The dust cloud responsible for infrared emission at the time of IRAS did not cause a deep optical decline of which none have been seen for 60 years. Bogdanov et al.’s (2010) survey of JHKLM for 25 years from 1984 show a major IR excess present and weakening at the time of the IRAS observations with two weaker episodes in subsequent years. Bogdanov et al.’s KLM magnitudes from 1984 are acceptably fit by the blackbody fit to the reddening-corrected IRAS fluxes (Figure 6).

RT Nor: RT Nor closely resembles Y Mus in terms of its low covering factors at the time of the IRAS and Spitzer observations. RT Nor has experienced (according to AAVSO records) only three or four optical declines of three or more magnitudes in the last 50 years. None of the declines happened a few years prior to the IRAS or Spitzer observations. As in the case of Y Mus, we suppose that RT Nor is simply an infrequent producer of dust.

WX CrA: In contrast to Y Mus, UV Cas, and RT Nor, WX CrA is frequently in decline; for example, in the thirteen years from late-1992 to late-2005 it was almost always below maximum light, often by two or more magnitudes. The Spitzer observation acquired at maximum light was preceded by about three years at maximum light. The IRAS observations were similarly acquired at maximum light and preceded by about a decade without optical

declines according to AAVSO records and Feast et al. (1997). Thus, the greater IRAS fluxes and higher covering factor ($R = 0.49$ versus $R = 0.14$) relative to Spitzer fluxes must be due to ejections of dust off the line of sight. Then, the fact that both R values are fairly representative values suggests that ejection of puffs occurs about as frequently as optical declines, i.e., there is no strong directional dependence for ejection of puffs.

RY Sgr: Infrared emission from RY Sgr provides higher covering factors than found for WX CrA suggesting a higher dust ejection rate. At the time of the Spitzer observations, RY Sgr was in decline but the covering factor R was only 0.20. An above average R ($=0.76$) was found from the IRAS observations. Major optical declines occur at a frequency of about one every five years. A distinguishing mark of RY Sgr is its periodic Cepheid-like variation in optical light and the consequent variation in the infrared emission by the dust which is heated by optical light (Feast et al. 1997; Feast 1979, 1986). The amplitude of the effect at L is about 0.8 magnitudes or a factor of two. Without a correction for this pulsational variation, comparison of IRAS and Spitzer fluxes are not immediately interpretable solely in terms of dust ejection episodes. Nevertheless, we suggest that RY Sgr behaves similarly to WX CrA in terms of dust emission.

4.2. Covering factors and frequency of declines

There is a not unexpected correlation between the covering factor R and the frequency of declines. As a measure of the latter, we use the inter-fade period ΔT (in days) determined by Jurcsik (1996). In Figure 13, we show ΔT versus R . Apart from the hot RCB MV Sgr, R appears independent of ΔT for values of $\Delta T > 2000$ days but increases steeply with decreasing ΔT below 2000 days. The mean ΔT for stars with $R < 0.30$ is 5600 days from 13 stars with the subset of 5 stars with $R < 0.10$ giving a mean $\Delta T = 10300$ days. For $R < 0.30$, the mean is $\Delta T = 1000$ days from 7 stars.

The simplest interpretation of this correlation is that the inter-fade period is roughly the time between ejection of puffs from all or most parts of the star and that these puffs take on the order of 2000 days to move out to distances where the dust temperature is lower than about 100 K. Ten stars in Table 3 were not studied by Jurcsik. Of these, the data on V magnitudes in the last 9 years for six stars (V1783 Sgr, V1157 Sgr, V739 Sgr, ES Aql, FH Sct, and V517 Oph) are available in the ASAS-3 database and appear to be consistent with the correlation suggested by Figure 13. With the exception of V1783 Sgr (with $\Delta T \sim 1000$ days), the other five stars are frequently in decline (at least 5 declines in the last 9 years). The data for the other four stars (Z Umi, MACHOJ181933, DY Per, and HV 2671) are too sparse to estimate their ΔT .

4.3. On the back of an envelope

As a guide to aspects of the infrared emission by dust in the circumstellar shell, the following back-of-an-envelope calculations are offered.

The equilibrium temperature of a grey dust grain ($T_d(r)$) in an optically thin circumstellar environment is given by

$$T_d(r) = \left(\frac{R_*}{2r}\right)^{0.5} T_* \quad (1)$$

where R_* is the stellar radius, r is the radial distance from the stellar center, and T_* is the stellar blackbody temperature (Kwok 2007, p.314, eqn. 10.32). For $T_* = 6000$ K, a representative temperature for a warm RCB, the dust temperature is 1320 K at 10 stellar radii and falls to 500 K at 50 stellar radii. This temperature at 10 stellar radii is close to the condensation temperature of carbon soot. The temperature at 50 stellar radii is fairly typical of the warm blackbody temperature from the fit to the Spitzer spectra.

If the velocity of the dust is expressed in units of 10 km s^{-1} and the radius of the star in units of 100 solar radii, the time for dust to travel out from a distance r_i/R_* to r_f/R_* is given by

$$t = 0.22 \frac{R_{100}}{v_{10}} \left[\frac{r_f}{R_*} - \frac{r_i}{R_*} \right] \quad (2)$$

where t is expressed in years. For example, dust moving at 10 km s^{-1} will take about 10 years to move from 10 to 50 stellar radii assuming the RCB radius is about 100 solar radii which is representative of yellow supergiants like the RCBs. A velocity of 10 km s^{-1} is a typical value for circumstellar gas around normal dusty AGB stars. Very blue-shifted components to the Na D lines are seen at the time of recovery from a deep minimum - say, 300 km s^{-1} (Rao et al. 1999). The evolution of the RCB spectra and lightcurves during declines are consistent with dust that forms close to the stellar atmosphere and then is accelerated to hundreds of km s^{-1} by radiation pressure (e.g., Clayton et al. 1992; Whitney et al. 1993). There is also some evidence that the strength of the blue shifted absorption seen in He I 10830 Å is inversely correlated with time since the last decline (Geballe et al. 2009; Clayton et al. 2011, in preparation). At present, the location of this gas and its relation to the thinning puff are unknown. However, our results indicate that the dust detected at the Spitzer and IRAS wavelengths is expanding at may be tens of km/s but not hundreds (see below). In deep declines, the photospheric spectrum is often ‘washed out’, an effect attributed to scattering of photospheric light off the puffs in the circumstellar environment. There is no direct way

to measure the velocity of the dust because of the lack of sharp spectroscopic features that provide radial velocities. Indeed, the nearest method to measure the velocity of the dust is to study the dust scattered photospheric spectrum of the star by moving (expanding) dust cloud. Such a model has been shown by Herbig (1969), Kwok (1976), and in a more detailed way by Van Blerkom & Van Blerkom (1978), where they show the change in profiles of stellar absorption lines by expanding dust and the redshifts expected. We have measured such redshifts of the absorption lines in three minima of R CrB including the current one. Our KECK high-resolution (30,000), high S/N spectra obtained when the star is at $V \sim 15^{\text{th}}$ show the scattered stellar absorption spectrum very clearly and redshifts of about 25 km s^{-1} relative to the mean radial velocity of the star at maximum light, suggesting dust velocities of this order. We have also broadened the normal light maximum spectrum and matched to the scattered spectrum with such velocities, suggesting also that dust is expanding at maybe tens of km s^{-1} but not hundreds (Rao & Lambert, in preparation). Thus, if the puffs are moving radially away from the star, an expansion velocity of $10\text{-}20 \text{ km s}^{-1}$ seems to be well justified. Bogdanov et al. (2010) - by using calculations where the momentum couple the gas and dust in a self-consistent procedure - estimate the characteristics of the stellar wind due to radiation pressure on the dust in two RCBs. Consistently, with our suggested expansion velocity, they compute gas and dust expansion rates of 8.8 and 15.6 km s^{-1} for the RCBs UV Cas and SU Tau, respectively, supporting our independent estimation of the dust expansion velocity in RCBs and suggesting that the dust detected by Spitzer and IRAS may not be close to the star where dust formation seems to occur. Finally, note that with dust cloud complex motions of $10\text{-}20 \text{ km s}^{-1}$ and assuming a distance of 2 kpc , the $18'$ diameter cool (30 K , at wavelengths beyond $60 \mu\text{m}$) dust shell seen around R CrB (Rao & Nandy 1986; Guillet et al. 1986) would have left the star 256000 years ago. Thus, this cool dust component may be the remnant of the stage when R CrB was a red giant for the first time (Rao & Nandy 1986).

Thus, a RCB experiencing infrequent ejections of dust would be expected to show significant variations in infrared flux on timescales of a decade or two, i.e., differences should be seen in comparing IRAS and Spitzer fluxes for those stars which rarely emit puffs. Conversely, stars ejecting puffs at a rate much shorter than this timescale should show a quasi-constant infrared excess where the covering factor will depend in part on the total solid angle subtended by puffs which in turn will depend on the number of ejection sites close to the stellar surface and the angular expansion of a puff as it moves away from the star.

These order of magnitude estimates for dust temperature and timescale may be tested using the RCBs which are extreme outliers in the histogram of the IRAS to Spitzer $12 \mu\text{m}$ flux ratios. These are stars for which one might expect a single puff to be present at a given time and, hence the same puff may have been observed by IRAS and Spitzer. Two tests are

offered.

First, equations (1) and (2) may be combined to express the timescale t in terms of the blackbody temperatures from the IRAS and the Spitzer fluxes. Assuming $r_{100}/v_{10} = 1$ and taking the temperatures from Table 3, we predict a timescale of 13, 20, and 28 years for UV Cas, Y Mus, and RT Nor, respectively, the three stars with the most extreme decrease in $12 \mu\text{m}$ flux from IRAS to Spitzer. These estimates are very similar to the time interval of about 25 years between the IRAS and Spitzer observations. For the other two outliers, both with less extreme ratios of the ratio of IRAS to Spitzer fluxes, the estimated timescale is much less than the 25 year time interval but this may be due to their higher frequency of puff ejection and, hence, the presence in the circumstellar shell of more than a single puff.

The second test uses the derived covering factors and the change in these factors between the IRAS and Spitzer observations. On the assumption that the physical size of the puff is not changing, the covering factor R and dust temperature T_d are related as $R \propto T_d^4$. For the three most extreme outliers in the IRAS to Spitzer flux ratio distribution, the ratio of R factors and the ratio of T_d^4 are in fair accord: the R -ratio and T_d^4 -ratios are 11 and 6, 8 and 5, and 8 and 6 for UV Cas, Y Mus, and RT Nor, respectively. Again, the indication is that a single puff present at the time of the IRAS observations remained unaccompanied at the time of the Spitzer observations but had been driven to a larger radial distance.

This test may be applied to the entire sample including outliers. In Figure 14, the ratio of the Spitzer to IRAS blackbody temperatures is plotted versus the ratio of the covering factors. Given their characteristic optical variability, it is remarkable that the RCB stars form a rather well defined trend in this figure. On the assumption, as above, that the physical size of a puff does not change as it moves away from its star, the $R \propto T_d^4$ may be applied to the sample and provides the evolutionary track shown on Figure 14. Stars near the point corresponding to equal ratios in T_d and in R are identified as stars whose circumstellar environment was essentially unchanged between the IRAS and Spitzer observations. The extremity of the trend is set by the three extreme outliers (UV Cas, Y Mus, and RT Nor) for which we have suggested the principal puff present at the time of the IRAS observations evolved away from the star to greater distances and, therefore, a lower covering factor and a lower temperature. An interpretation of the fact that many stars connect the normalization point and the location of the extreme outliers is that for these stars too the principal puffs present for IRAS remained the principal puffs for Spitzer but then at a greater distance. Of course, this interpretation has the novel, if uncomfortable conclusion, that the majority of our collection of RCBs is now experiencing a decline in their propensity to eject puffs of soot. Since the trend is anchored by three extreme outliers, it is challenging to identify systematic errors in either the IRAS or Spitzer data that might account for the uncomfortable

conclusion.

A key question about the formation and ejection of the dusty puffs is whether there is a preferred location for their formation with respect to the star. (Their ejection path is presumed to be radially outward above the point of formation.) We consider a few limiting cases.

There is a preferred location for puff formation: One imagines, for example, such possibilities as active regions at one or both rotational poles, along a latitudinal belt, or a long-lived active region (e.g., Wdowiak 1975; Soker & Clayton 1999). The covering factor will likely be small for ejection from a single active region but larger for fairly uniformly active latitudinal belt.

In this circumstance, optical declines will be less frequent than the time between ejection of puffs unless the preferred direction intersects the line of sight to the star. In the extreme case, the RCB will show an infrared excess but very rarely or never an optical decline.

If time between fresh puffs is long, the infrared excess will move from near- to far-infrared wavelengths before ejection of a fresh puff, i.e., there will be large variations in flux at L and at Spitzer/IRAS wavelengths.

At the other extreme when puffs are ejected frequently, the star will show smaller variations in infrared excess with a broader distribution in infrared wavelengths.

The outliers such as UV Cas, Y Mus, and RT Nor are candidates for puff ejection occurring – currently – from an active region which ejects puffs off the line of sight. This region may or may not represent a preferred location in the long-term. Rao & Raveendran (1993) have suggested a preferred plane for dust around V854 Cen from polarimetry during two deep minima. Clayton et al. (1997) from their spectro-polarimetric observations of R CrB in a deep minimum suggested a dust disk or torus that obscure the star with diffuse dust above the poles. On the other hand, resolved dust shells around RCBs at visible and infrared wavelengths suggest different shapes ranging from spherical symmetry to slightly elliptical (Guillet et al. 1986; Walker 1986; Clayton et al. 1999; Bright et al. 2011). Thus preferred locations are a possibility in some cases and under some circumstances.

Puff ejection occurs from regions distributed isotropically over the stellar surface: If the number of active regions is small and ejection of puffs infrequent, there will be large variations in the infrared excess and long intervals between optical declines with possibly a low covering factor. This state of affairs is generally equivalent to that expected from a preferred location for puff ejection lying off the line of sight. Again, the outliers such as UV Cas and friends fall in this category.

At the other extreme, the active regions may be many and puff ejection very frequent, the infrared variations will be small, the optical decline rate will be high and the covering factor high. These circumstances describe well a majority of the RCBs studied here.

These conclusions drawn from Spitzer and IRAS flux similarities and differences echo those given earlier by Feast et al. (1997) from their two decades of JHKL photometry of about a dozen RCBs. The J magnitude is set by the stellar flux and is sensitive to optical declines. The L magnitude monitors the dust emission, especially the warm and presumably freshly-formed dust; Feast (1997) suggests there is no evidence for dust warmer than about 1500 K. Not surprisingly, the L magnitude of a given RCB is variable with an amplitude of up to three magnitudes with larger L variations associated with the longer timescales. There is a very approximate tendency for the larger L variations to come from stars with the longer inter-fade periods, a correlation consistent with our observation that the larger covering factors are paired with the shorter inter-fade periods. Significantly, Feast et al. (1997) conclude that ‘models involving fixed geometry for the ejection of dust from the star appear to be ruled out and the data support the random dust-puff model.’ This remark derived from the dust as measured by the L magnitudes refers pretty directly to the formation of fresh dust quite close to a star.

5. Dust around RCBs in different environments

How different or similar is the dusty circumstellar shell around RCB stars in different environments (e.g., at different metallicities) such as the solar neighbourhood and the Large Magellanic Cloud?

The properties of dust around RCBs in the Large Magellanic Cloud (LMC) have been explored by Tisserand et al. (2009) using the photometry from Spitzer IRAC and MIPs bands. In various diagnostic diagrams such as the [24.0] absolute magnitude versus the [8.0]–[24.0] color (as estimated from Spitzer mid-IR bands and the LMC’s distance modulus), the LMC cool (i.e, DY Per-like), warm and hot RCBs are distinguishable. The DY Per-like dust shells have the bluest colors and lowest absolute magnitudes with the hotter stars trending to higher absolute magnitudes and redder colors.

For the RCBs in our sample, we obtained monochromatic fluxes at 8.0 and 24.0 μm from the reddening-corrected Spitzer spectra. We obtained magnitudes in the system of IRAC [8.0] and MIPs [24.0] μm by using the appropriate flux calibrations (Engelbracht et al. 2007) and IRAC manuals. It is to be noted that our [8.0] and [24.0] magnitudes are not band averaged as is the standard photometry used by Tisserand et al. (2009). However,

systematic effects between our magnitudes and those from Tisserand et al. (2009) are thought to be small. For the few stars where our Spitzer spectrum does not extend to $8\ \mu\text{m}$, we used the blackbody fits that characterize the observed spectrum (Section 3) to estimate the flux at $8\ \mu\text{m}$. In addition, for stars like V854 Cen and DY Cen where the $6\text{--}10\ \mu\text{m}$ emission features dominate the spectra, we used the emission free continuum flux at the appropriate wavelengths.

For our comparison with the LMC’s RCBs, we must estimate the distances to the local RCBs. We have assumed $M_{bol} = -5.0 \sim M_V$ for most of the stars, with the exception of the cooler RCBs (see below). Individual distances are estimated from the reddening-corrected V magnitudes from which M_{bol} at 8 and $24\ \mu\text{m}$ were obtained. For DY Per, the distance of 2.7 kpc as estimated by Začs et al (2007) has been adopted. Tisserand et al. (2009) show that the M_V of RCBs in the LMC change from -5 to -3.4 as a function of the V-I color, particularly for V-I between 0.6 and 1.5 (their Figure 3), suggesting that cooler RCBs have lower M_V s. We have used the V-I color of the cooler RCBs in our sample to obtain M_V estimates except for U Aqr and MACHOJ181933. These estimates are used in determining the distances to the individual stars and these distances are in turn used in estimating the absolute magnitude at 24 microns. U Aqr is a halo star and the M_V of -5 seems to be justified (Cottrell & Lawson 1998). MACHOJ181933 displays the largest V-I color in our sample and we have assumed $M_V = -5.0$ for this star. This is because Tisserand et al. (2009) show that there is not a unique relation between M_V and V-I color for V-I colors greater than 1.5 .

Figure 15 shows our sample of Galactic RCBs in the $[24.0]$ -absolute magnitude versus the $[8.0]\text{--}[24.0]$ color index plane, along with the LMC RCBs studied by Tisserand et al. (2009). The latter data were taken from Table 6 of Tisserand et al. (2009), in which a distance modulus of 18.5 was used for the LMC objects.

The only DY Per-like object in our sample is DY Per itself which merges with the the LMC DY Per-like objects, suggesting that the distance estimate of DY Per is not too much off. The other LMC RCBs and Galactic RCBs merge in this plot over the total range, suggesting that the dusty circumstellar shells are of similar nature. At the highest $[24.0]\ \mu\text{m}$ luminosities are found the hot RCBs and the Galactic center cool RCB MACHOJ181933 at $M([24.0]) = -14.37$. However, if we assume a distance modulus of 14.4 for the Galactic Center, then the $[24.0]\ \mu\text{m}$ luminosity is reduced to -11.06 (see Figure 15), which is consistent with the other RCBs in our sample and implying that M_V is not -5.0 for MACHOJ181933. Tisserand et al. (2009) found that M_V of RCBs extend from -5.2 to -3.4 or even -2.6 . The RCBs UV Cas, Y Mus, and RT Nor along with W Men (denoted as W in Figure 15) lie far below the $[24.0]\ \mu\text{m}$ magnitude of other RCBs although they have similar $[8.0]\text{--}[24.0]$ colors. This suggests that these stars have lower than average dust content. Indeed, UV CAs, Y

Mus, and RT Nor are just the three outliers (showing the highest IRAS/Spitzer flux ratios; see Section 4) displaying the lowest (0.01–0.035) covering factors in our sample, being very poor producers of dust. In short, we conclude that RCBs in the LMC and the Galaxy have similar dusty circumstellar shells.

6. Conclusions

Our almost-complete sample of Spitzer/IRS spectra of R Coronae Borealis stars has been combined with multi-color photometry of a RCB at maximum light to provide a spectral energy distribution from, in general, the U or V band to $37\ \mu\text{m}$. Each SED has been fit with a blackbody to represent the stellar flux and one, two, or three blackbodies to represent the emission from the circumstellar dust. A typical RCB emits about 30% of the stellar flux in the infrared. Although not discussed in this paper, emission features superimposed on the combination of dust blackbodies are with but a couple of exceptions limited to emission from 6-10 μm . The exceptions discussed by García-Hernández et al. (2011) are DY Cen and V854 Cen where emission is from PAHs and C_{60} molecules.

For the majority of the RCBs, there is fair agreement between the Spitzer spectrum and the 12 μm and 25 μm fluxes from IRAS from about three decades previously. There are five exceptions where the IRAS fluxes are between three to five times those recorded by Spitzer. Oddly, these outliers do not have counterparts for which the IRAS fluxes are lower than the Spitzer values.

Our results are consistent with the proposal that clouds of carbon soot form in puffs above the surface of a RCB. There is evidence that puffs are formed randomly and without a preferred direction. For some stars and especially for the above five outliers a single puff may dominate the infrared emission. Our sample of Galactic RCBs and those in the LMC share the same properties of their dusty circumstellar shells, as evidenced by their total 24 μm luminosity and [8.0]–[24.0] color index.

Although an important next step is to attempt modeling the radiative transfer in the dusty circumstellar environment for our sample of RCB stars, the value of long-term monitoring through infrared photometry and spectroscopy should not be underestimated.

We would like to thank the referee G. C. Clayton for suggestions that help to improve the paper. We thank Michael Feast, Patricia Whitelock and Fred van Wyk at the SAAO for observing stars at the time of our Spitzer observations. We thank too N.M. Ashok of PRL, Ahmedabad for observing several RCB stars at the Gurushikhar Observatory. We thank

John Lacy and Amanda Bayless for discussions about modeling the dusty environment of RCB stars. D.A.G.H. acknowledges support for this work provided by the Spanish Ministry of Science and Innovation (MICINN) under the 2008 Juan de la Cierva Programme and under grant AYA-2007-64748. N.K.R. would like to thank A. V. Raveendran for his help. D.L.L. acknowledges support for this work provided by NASA through an award for program GO #50212 issued by JPL/Caltech and the Robert A. Welch Foundation of Houston, Texas through grant F-634. Extensive use has been made of the AAVSO's database of observations of RCB stars; we are most grateful to the many observers who have and continue to contribute to this record of the stars' variability. This work is based on observations made with the Spitzer Space Telescope, which is operated by the Jet Propulsion Laboratory, California Institute of Technology, under NASA contract 1407. Part of this work is based on observations made with the IAC-80 telescope under the Spanish Instituto de Astrofísica de Canarias Service Time. The IAC-80 is operated by the Instituto de Astrofísica de Canarias in the Observatorio del Teide.

Facilities: Spitzer: IRS; IAC80: Camelot; SAAO: .

REFERENCES

- Alcock, C., Allsman, R. A., Alves, D. R. et al. 2001, ApJ, 554, 298
- Alksnis, A., Larionov, V.M., Smirnova, O., Arkharov, A.A., Konstantinova, T.S., Larionova, L.V., & Shenavrin, V.I. 2009, BaltA, 18, 53
- Asplund, M., Gustafsson, B., Kiselman, D., & Eriksson, K. 1997, A&A, 318, 521
- Asplund, M., Gustafsson, B., Rao, N.K., & Lambert, D.L. 1998, A&A, 332, 651
- Asplund, M., Gustafsson, B., Lambert, D. L., & Rao, N. K. 2000, A&A, 353, 287
- Beichman, C.A., Neugebauer, G., Habing, H.J., Clegg, P.E., & Chester, T.J. 1988, Infrared Astronomical Satellite (IRAS) Catalogs and Atlases, Vol. 1: Explanatory Supplement (Washington:NASA)
- Benson, P.J., Clayton, G.C., Garnavich, P., & Szkody, P. 1994, AJ, 108, 247
- Bergeat, J., Knapik, A., & Rutily, B.D. 1999, A&A, 342, 773
- Bogdanov, M.B., Taranov, O.G., & Shenavrin, V.I. 2010, Astr. Reports, 54, 620
- Bond, H.E., Luck, R.E., & Newman, M.J. 1979, ApJ, 233, 205

- Bright, S. N., Chesneau, O., Clayton, G. C., De Marco, O., Leo, I. C., Nordhaus, J., Gallagher, J. S. 2011, MNRAS (in press; astro-ph/1102.4147)
- Cardelli, J. A., Clayton, G. C., & Mathis, J. S. 1989, ApJ, 345, 245
- Carter, B.S. 1990, MNRAS, 242, 1
- Chiar, J. E., & Tielens, A. G. G. M. 2006, ApJ, 637, 774
- Clayton, G. C., Whitney, B. A., Stanford, S. A., Drilling, J. S. 1992, ApJ, 397, 652
- Clayton, G.C., Kelly, D.M., Lacy, J.H., Little-Marenin, I.R., Feldman, P.R., & Bernath, P.F. 1995, AJ, 109, 2096
- Clayton, G. C. 1996, PASP, 108, 225
- Clayton, G. C., Bjorkman, K. S., Nordsieck, K. H., Zellner, E. B., Schulte-Ladbeck, R. E. 1997, ApJ, 476, 870
- Clayton, G.C., Kerber, F., Gordon, K.D., Lawson, W.A., Wolff, M.J., Pollacco, D.L., & Furlan, E. 1999, ApJ, 517, L143
- Clayton, G. C., Hammond, D., Lawless, J., Kilkenny, D., Evans, T. L., Mattei, J., Landolt, A. U. 2002, PASP, 114, 846
- Clayton, G.C., Herwig, F., Geballe, T.R., Asplund, M., Tenenbaum, E.D., Engelbracht, C.W., & Gordon, K.D. 2005, ApJ, 623, L141
- Clayton, G.C., Geballe, T.R., Herwig, F., Fryer, C. & Asplund, M. 2007, ApJ, 662, 1220
- Clayton, G.C., De Marco, O., Whitney, B. A., Babler, B., Gallagher, J. S., Nordhaus, J., Speck, A. K., Wolff, M. J., Freeman, W. R., Camp, K. A., Lawson, W. A., Roman-Duval, J., Misselt, K. A., Meade, M., Sonneborn, G., Matsuura, M., Meixner, M. 2011, AJ (in press)
- Colangeli, L., Mennella, V., Palumbo, P., Rotundi, A., Bussoletti, E. 1995, A&AS, 113, 561
- Cottrell, P.L., & Lambert, D.L. 1982, The Observatory, 102, 149
- Cox, N. L. J., García-Hernández, D. A., García-Lario, P., Manchado, A. 2011, AJ, 141, 111
- Crause, L.A., Lawson, W.A., & Henden, A.A. 2007, MNRAS, 375, 301
- Cutri, R. M., et al., 2003, The 2MASS All-Sky Point Source Catalog, VizieR Online Catalog, 2246, 0

- Danziger, I.J., 1965, MNRAS, 130, 199
- de Laverny, P., & Mékarnia, D. 2004, A&A, 428, L13
- De Marco, O., Clayton, G. C., Herwig, F., Pollacco, D. L., Clark, J. S., Kilkenny, D. 2002, AJ, 123, 3387
- Engelbracht, C. W. et al. 2007, PASP, 119, 994
- Feast, M.W. 1979, in IAU Colloq. 46, Changing Trends in Variable Star Research, ed. F.M. Bateson, J. Smak, & I.M. Urch (Hamilton: Univ. Waikato) 246
- Feast, M.W., in IAU Colloq. 87, Hydrogen Deficient Stars and Related Objects, ed. K. Hunger, D. Schönberner, & N.K. Rao (Dordrecht: Reidel) 151
- Feast, M.W. 1996, in ASP Conf. Ser. 96, Hydrogen Deficient Stars, ed. C.S. Jeffery & U. Heber (San Francisco:ASP) 3
- Feast, M.W. 1997, MNRAS, 285, 339
- Feast, M.W., & Glass, I.S. 1973, MNRAS, 161, 293
- Feast, M. W., Carter, B. S., Roberts, G., Marang, F., Catchpole, R. W. 1997, MNRAS, 285, 317
- Fernie, J.D., Sherwood, V., & DuPuy, D.L. 1972, ApJ, 172, 383
- Fitzgerald, M.P. 1968, AJ, 73, 683
- Forrest, W. J., Gillett, F. C., & Stein, W. A. 1972, ApJ, 178, L17
- García-Hernández D. A., Perea-Calderón, J. V., Bobrowsky, M., García-Lario, P. 2007, ApJ, 666, L33
- García-Hernández D. A., Perea-Calderón, J. V., Engels, D., García-Lario, P. 2009 in “Asymmetrical Planetary Nebulae IV”, p. 325
- García-Hernández D. A., Hinkle, K. H., Lambert, D. L., Eriksson, K. 2009, ApJ, 696, 1733
- García-Hernández D. A., Lambert, D. L., Rao, N. K., Hinkle, K. H., Eriksson, K. 2010, ApJ, 714, 144
- García-Hernández D. A., Rao, N. K., & Lambert, D. L. 2011, ApJ, 729, 126
- Gaustad, J.E., Stein, W.A., Forrest, W.J., & Pipher, J.L. 1988, PASP, 100, 388

- Geballe, T. R., Rao, N. K., & Clayton, G. C. 2009, *ApJ*, 698, 735
- Gillett, F. C., Backman, D. E., Beichman, C., & Neugebauer, G. 1986, *ApJ*, 310, 842
- Glass, I.S. 1978, *MNRAS*, 185, 23
- Goldsmith, M.J., Evans, A., Albinson, J.S., & Bode, M.F. 1990, *MNRAS*, 245, 119
- Goswami, A., Rao, N.K., & Lambert, D.L. 1997, *PASP*, 109, 796
- Heck, A., Houziaux, L., Manfroid, J., Jones, D.H.P., & Andrews, P.J. 1985, *A&AS*, 61, 375
- Herbig, G. H. 1969, *Mém. Soc. Roy. Sc Liege*, 19, 13
- Higdon, S. J. U. et al. 2004, *PASP*, 116, 975
- Hoffleit, D. 1959, *AJ*, 64, 241
- Houck, J. R. et al. 2004, *ApJS*, 154, 18
- Jeffery, C.S., Heber, U., Hill, P.W., & Pollacco, D. 1988, *MNRAS*, 231, 175
- Jeffery, C. S., & Heber, U. 1993, *A&A*, 270, 167
- Jeffery, C.S. 1995, *A&A*, 297, 779
- Jeffery, C. S., Karakas, A. I., & Saio, H. 2011, *MNRAS* (in press)
- Jurcsik, J. 1996, *Acta Astron.*, 46, 325
- Kilkenny, D., & Whittet, D.C.B. 1984, *MNRAS*, 208, 25
- Kilkenny, D., Coulson, I.M., Laing, J.D., Spencer Jones, J. & Engelbrecht, C. 1985, *SAAO Circ.*, 9, 87
- Kilkenny, D., Lloyd Evans, T., Bateson, F. M., Jones, A. F., Lawson, W. A. 1992, *The Observatory*, 112, 158
- Kipper, T., & Klochkova, V.G. 2006, *BaltA*, 15, 531
- Kwok, S. 1976, *JRASC*, 70, 49
- Kwok, S. 2007, *Physics and Chemistry of the Interstellar Medium*, (Sausalito:University Science Books)
- Lambert, D. L., & Rao, N. K. 1994, *JApA*, 15, 47

- Lambert, D. L., Rao, N. K., Pandey, G., Ivans, I. I. 2001, *ApJ*, 555, 925
- Lawson, W.A., Cottrell, P.L., Kilmartin, P.M., & Gilmore, A.C. 1990, *MNRAS*, 247, 91
- Lawson, W. A., & Cottrell, P.L. 1997, *MNRAS*, 285, 266
- Lawson, W.A. et al. 1999, *AJ*, 117, 3007
- Leão, I. C., de Laverny, P., Chesneau, O., Mékarnia, D., de Medeiros, J. R. 2007, *A&A*, 466, L1
- Lloyd Evans, T., Kilkenny, D., van Wyk, F. 1991, *The Observatory*, 111, 244
- Marang, F., Kilkenny, D., Menzies, J.W., & Spencer Jones, J.H. 1990, *SAAO Circ.*, 14, 1
- Pandey, G., & Lambert, D. L. 2011, *ApJ*, 727, 122
- Pollacco, D.L., & Hill, P.W. 1991, *MNRAS*, 248, 572
- Pollacco, D. L., Hill, P. W., & Tadhunter, C. N., 1990, *MNRAS*, 245, 204
- Pollacco, D.L., Hill, P.W., Houziaux, L., & Manfroid, J. 1991, *MNRAS*, 248, 1p
- Pugach, A.E. 1977, *IBVS*, 1277, 1
- Rao, N.K. 1980, *The Observatory*, 100, 164
- Rao, N.K., Ashok, N.M., & Kulkarni, P.V. 1980, *JApA*, 1, 71
- Rao, N. K., & Raveendran, A. V. 1993, *A&A*, 274, 330
- Rao, N. K., Giridhar, S., & Lambert, D. L. 1993, *A&A*, 280, 201
- Rao, N. K. 1995, *BASI*, 23, 351
- Rao, N.K. et al. 1999, *MNRAS*, 310, 717
- Rao, N. K., & Lambert, D. L. 1993, *PASP*, 105, 574
- Rao, N. K., & Lambert, D. L. 2000, *MNRAS*, 313, L33
- Rao, N. K., Lambert, D. L., & Shetrone, M. D. 2006, *MNRAS*, 370, 941
- Rao, N. K., & Lambert, D. L., 2008, *MNRAS*, 384, 477

- Rao, N. K., & Lambert, D. L., 2010, in *Recent Advances in Spectroscopy: Theoretical, Astrophysical and Experimental Perspectives*, ed. R.J. Chaudhuri, M.V. Mekkaden, A.V. Raveendran, & A.S. Narayanan (Berlin: Springer) 177
- Rao, N. K., & Nandy, K. 1986, *MNRAS*, 222, 357
- Rosenbush, A.E. 1995, *AN*, 316, 213
- Scott, A. D., Duley, W. W., & Jahani, H. R. 1997a, *ApJ*, 490, L175
- Siedel, Th. 1957, *Mitt. Veränderliche Sterne*, Nr. 244
- Soker, N., & Clayton, G. C. 1999, *MNRAS*, 307, 993
- Soszyński, I. et al. 2009, *AcA*, 59, 335
- Stein, W. A., Gaustad, J., Gillett, F. C., Knacke, R. F. 1969, *ApJ*, 155, L3
- Strecker, D.W. 1975, *AJ*, 80, 451
- Tenenbaum, E.D. et al. 2005, *AJ*, 130, 256
- Tisserand, P. et al. 2009, *A&A*, 501, 985
- Tokunaga, A.T. 2000, *Allen's Astrophysical Quantities*, ed. A.N. Cox (4th edn. New York:Springer,)
- van Blerkom, J., & van Blerkom, D. 1978, *ApJ*, 225, 482
- Vanture, A.D., Zucker, D., & Wallerstein, G. 1999, *ApJ*, 514, 932
- Walker, H. J. 1986, in *IAU.Coll. 87, Hydrogen Deficient Stars & Related Objects*, ed. K. Hunger, D. Schönberner, & N.K. Rao (Dordrecht:Reidel) 407
- Wdowiak, T. J. 1975, *ApJ*, 198, L139
- Werner, M. et al. 2004, *ApJS*, 154, 1
- Whitney, B. A., Balm, S. P., & Clayton, G. C. 1993, *ASPC*, 45, 115
- Woitke, P., Goeres, A., & Sedlmayr, E. 1996, *A&A*, 313, 217
- Yakovina, L.A., Pugach, A.F. & Pavlenko, Ya.V. 2009, *Astr. Reports*, 53, 187
- Začs, L., Mondal, S., Chen, W. P., Pugach, A. F., Musaev, F. A., Alksnis, O. 2007, *A&A*, 472, 247

Zaniewski, A., Clayton, G.C., Welch, D.L., Gordon, K.D., Minniti, D., & Cook, K.H. 2005, AJ, 130, 2293

Zavatti, F. 1975, IBVS, 1027, 1

Zhilyaev, B.E., Orlov, M.Ya., Pugach, A.F., Rodrigues, M.G., & Totochava, A.G. 1978, R Coronae Borealis-type stars, (Naukova dumka: Kiev)

Table 1. The RCB stars sample^a

RCB star	RA _{J2000}	DEC _{J2000}	Category	F ₁₂ [Jy]	F ₂₅ [Jy]	Obs. Date yyyy/mm/dd	Var. ^b	Modules	Program #
UV Cas	23:02:14.62	+59:36:36.6	A	3.81	1.28	2008/08/12	max	SL,SH,LH	50212
S Aps	15:09:24.53	−72:03:45.1	C	2.71	1.02	2008/04/25	max	SL,SH,LH	50212
SV Sge	19:08:11.76	+17:37:41.2	C	3.29	1.66	2008/05/26	max	SL,SH,LH	50212
Z UMi	15:02:01.33	+83:03:48.6	C	2.12	0.82	2008/10/20	min[2]	SL,SH,LH	50212
V1783 Sgr	18:04:49.74	−32:43:13.4	C	3.20	1.26	2008/04/25	max	SL,SH,LH	50212
WX CrA	18:08:50.48	−37:19:43.2	C	2.31	0.77	2008/10/10	max	SL,SH,LH	50212
V3795 Sgr	18:13:23.58	−25:46:40.8	AB	4.17	1.80	2008/04/25	max	SL,SH,LH	50212
V1157 Sgr	19:10:11.83	−20:29:42.1	C	3.21	1.17	2008/06/02	min[2]	SL,SH,LH	50212
Y Mus	13:05:48.19	−65:30:46.7	A	1.02	0.35	2008/04/25	max	SL,SH,LH	50212
V739 Sgr	18:13:10.54	−30:16:14.7	C	1.27	0.36	2008/04/25	max	SL,SH,LH	50212
VZ Sgr	18:15:08.58	−29:42:29.4	AB	1.11	0.59	2008/04/25	min[4]	SL,SH,LH	50212
U Aqr	22:03:19.70	−16:37:35.2	C	1.11	0.51	2008/06/29	max	SL,SH,LH	50212
MACHOJ181933	18:19:33.75	−28:35:58.0	C	2008/04/25	max	SL,SH,LH	50212
ES Aql	19:32:21.61	−00:11:31.0	C	1.43	0.52	2008/05/27	max	SL,SH,LH	50212
FH Sct	18:45:14.84	−09:25:36.1	A	0.62	0.49	2008/06/02	max	SL,SH,LH	50212
SU Tau	05:49:03.73	+19:04:22.0	A	9.50	4.14	2008/04/28	max	SH,LH	50212
DY Per	02:35:17.13	+56:08:44.7	C	8.65	1.71	2008/09/13	max	SH,LH	50212
V517 Oph	17:15:19.74	−29:05:37.6	C	7.81	2.53	2008/04/25	min[2.4]	SH,LH	50212
V CrA	18:47:32.30	−38:09:32.3	AB	5.66	2.46	2005/09/14	max	SL,LL	7
RZ Nor	16:32:41.66	−53:15:33.2	A	3.45	1.75	2006/03/22	max	SL,LL	7
RT Nor	16:24:18.68	−59:20:38.6	A	0.93	0.40	2005/04/21	max	SL,LL	7
RS Tel	18:18:51.22	−46:32:53.4	A	1.54	0.71	2005/09/10	max	SL,LL	7
V482 Cyg	19:59:42.57	+33:59:27.9	A	0.98	0.41	2004/11/14	max	SL,LL	7
MV Sgr	18:44:31.97	−20:57:12.8	A	0.60	1.57	2005/04/18	max	SL,SH,LH	3362
RY Sgr	19:16:32.76	−33:31:20.4	A	77.20	26.20	2004/10/21	min[2.6]	SH,LH	3362
V854 Cen	14:34:49.41	−39:33:19.2	AB	23.00	7.82	2007/09/07	min[5.5]	SL,SH,LH	30077
UW Cen	12:43:17.18	−54:31:40.7	A	7.85	5.75	2008/08/17	max	SL,SH,LL	40061
DY Cen	13:25:34.08	−54:14:43.1	AB	0.91	0.93	2008/08/17	max	SL,LL	40061
R CrB	15:48:34.41	+28:09:24.3	A	17.10	3.94	2004/07/17	max	SH	93
V348 Sgr	18:40:19.93	−22:54:29.3	A	5.53	3.00	2006/10/22	min[2.7]	SL,LL	30380
HV 2671	05:33 48.94	−70:13:23.4	LMC-RCB	2006/11/14	...	SL,LL	30380

^aThe first 18 RCB stars were observed with Spitzer by us (Program #50212) while the rest of stars were observed by other programs and the data were retrieved from the Spitzer database (see text).

^bVariability status during the Spitzer observations; max: the star was observed at (or slightly below; e.g., <0.6–0.8 mag in V) maximum light. min: the star was observed during minimum light and the number between brackets indicate the V magnitudes below maximum.

Table 2. Optical and near infrared photometry^a

RCB star	Spitzer Obs. Date yyyy/mm/dd	IAC-80 Obs. Date yyyy/mm/dd	V/R/I ^b	SAAO Obs. Date yyyy/mm/dd	J/H/K/L
UV Cas	2008/08/12	2008/08/11 2008/08/13	10.73/9.86/9.01 10.72/9.86/8.99
S Aps	2008/04/25	2008/04/24	7.78/7.16/6.67/5.31
SV Sge	2008/05/26	2008/05/30	10.68/9.60/8.50
Z UMi	2008/10/20		
V1783 Sgr	2008/04/25	2008/04/24 2008/05/04	10.60/9.71/8.86 10.71/9.82/8.93	2008/04/29	8.74/8.34/7.96/...
WX CrA	2008/10/10		
V3795 Sgr	2008/04/25	2008/04/24 2008/05/04	11.57/10.94/10.27 11.57/10.94/10.29	2008/04/29	9.14/8.63/8.24/...
V1157 Sgr	2008/06/02	2008/06/03	13.20/12.23/11.23
Y Mus	2008/04/25		
V739 Sgr	2008/04/25	2008/04/24 2008/05/04	12.41/11.33/10.33 12.42/11.66/10.45	2008/04/29	10.11/9.49/8.70/...
VZ Sgr	2008/04/25		
U Aqr	2008/06/29	2008/06/26 2008/07/04	11.40/10.74/10.23 11.50/10.81/10.30
MACHOJ181933	2008/04/25	2008/04/24 2008/05/04	13.93/12.78/11.64 13.97/12.86/11.73		
ES Aql	2008/05/27	2008/05/30	12.28/11.17/10.09		
FH Sct	2008/06/02	2008/06/03	13.00/12.90/11.99		
SU Tau	2008/04/28	2008/04/23	9.79/ 9.15/ 8.56	2008/03/19	7.72/7.28/6.74/4.96
DY Per	2008/09/13		
V517 Oph	2008/04/25	2008/04/24 2008/05/04	14.05/12.51/10.96 13.73/12.25/10.74	2008/04/29	9.74/8.45/7.08/5.22

^aOptical and near infrared photometry for the RCB stars observed with Spitzer by us (Program #50212).

^bThe VRI magnitude errors are estimated to be of the order of ± 0.15 mag (see text).

Table 3. Blackbody fits to the RCB’s SEDs

RCB star	T_{star}	T_{BB1}	R_{BB1}	T_{BB2}	R_{BB2}	T_{BB1}	R_{BB1}	T_{BB2}	R_{BB2}	$E(B-V)^a$	ΔT^b
	(K)	(K)		(K)		(K)		(K)			(days)
		Spitzer				IRAS					
UV Cas	7200	510	0.03	180	0.001	800	0.28	0.90	25500
S Aps	4200	750	0.37	750	0.42	0.05	1400
SV Sge	4200	565	0.05	350	0.024	720	0.15	0.72	2500
Z UMi	5200	710	0.43	850	0.95	0.00	...
V1783 Sgr	5600	560	0.28	600	0.30	0.42	...
WX CrA	4200	575	0.15	120	0.006	700	0.49	0.06	2000
V3795 Sgr	8000	610	0.31	720	0.54	0.79	6000
V1157 Sgr	4200	770	0.59	120	0.007	850	1.01	0.30	...
Y Mus	7200	395	0.01	590	0.07	0.50	15300
V739 Sgr	5400	640	0.59	100	0.005	900	0.64	700	0.228	0.50	...
VZ Sgr	7000	700	0.17	140	0.008	700	0.17	140	0.008	0.30	1300
U Aqr	5000	475	0.23	140	0.021	560	0.37	0.05	1850
MACHOJ181933	4200	695	0.48	140	0.022	0.50	...
ES Aql	4500	700	0.49	700	0.49	0.32	...
FH Sct	6250	540	0.10	140	0.002	390	0.04	1.00	...
SU Tau	6500	635	0.45	635	0.50	0.50	1200
DY Per	3000	1400	0.31	1400	0.31	0.48	...
V517 Oph	4100	850	0.84	850	0.98	0.50	...
V CrA ^c	6500	550	0.38	150	0.020	1600	0.23	900	0.370	0.14	900
RZ Nor	5000	700	0.53	320	0.035	700	0.53	300	0.040	0.50	1100
RT Nor	6700	320	0.01	130	0.001	500	0.11	0.39	1950
RS Tel	6750	720	0.25	130	0.005	620	0.22	0.17	1200
V482 Cyg	4800	500	0.03	100	0.001	650	0.09	0.50	3400
MV Sgr	15400	1500	0.33	205	0.180	1500	0.33	235	0.236	0.43	6900
RY Sgr	7200	675	0.20	870	0.76	0.00	1400
V854 Cen	6750	900	0.32	140	0.030	1100	1.00	0.07	370
UW Cen ^d	7500	630	0.44	120	0.013	630	0.44	150	0.033	0.32	1100
DY Cen	19500	272	0.09	330	0.10	0.47	6400
R CrB	6750	950	0.30	680	0.20	0.00	1100
V348 Sgr	20000	707	0.63	100	0.035	707	0.63	100	0.035	0.45	560
HV 2671 ^e	20000	590	0.36	150	0.268	0.15	...

^aSee text for more details about the adopted E(B-V) values.

^bInter-fade periods from Jurcsick et al. (1996) (see also the text for more details).

^cAn additional 550 K blackbody with a covering factor of 0.37 is needed to fit the IRAS photometry.

^dAn additional very cool blackbody of 50 K with a covering factor of 0.05 is needed to fit the Spitzer data.

^eAn additional very cool blackbody of 40 K with a negligible covering factor is needed to fit the Spitzer data.

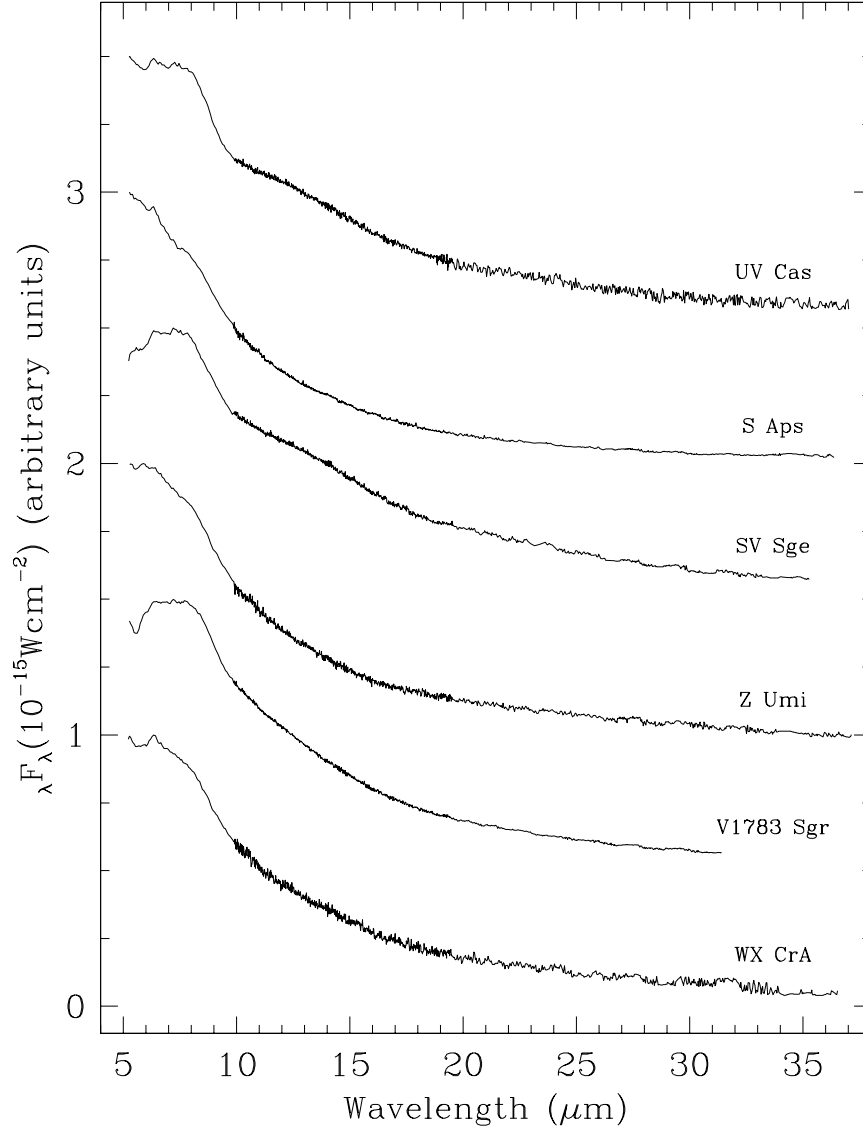


Fig. 1.— Spitzer/IRS reduced spectra over the full wavelength range $\sim 5\text{--}37 \mu\text{m}$ for (from top to bottom: UV Cas, S Aps, SV Sge, Z UMi, V1783 Sgr and WX CrA). Note that the spectra are normalized and displaced for clarity.

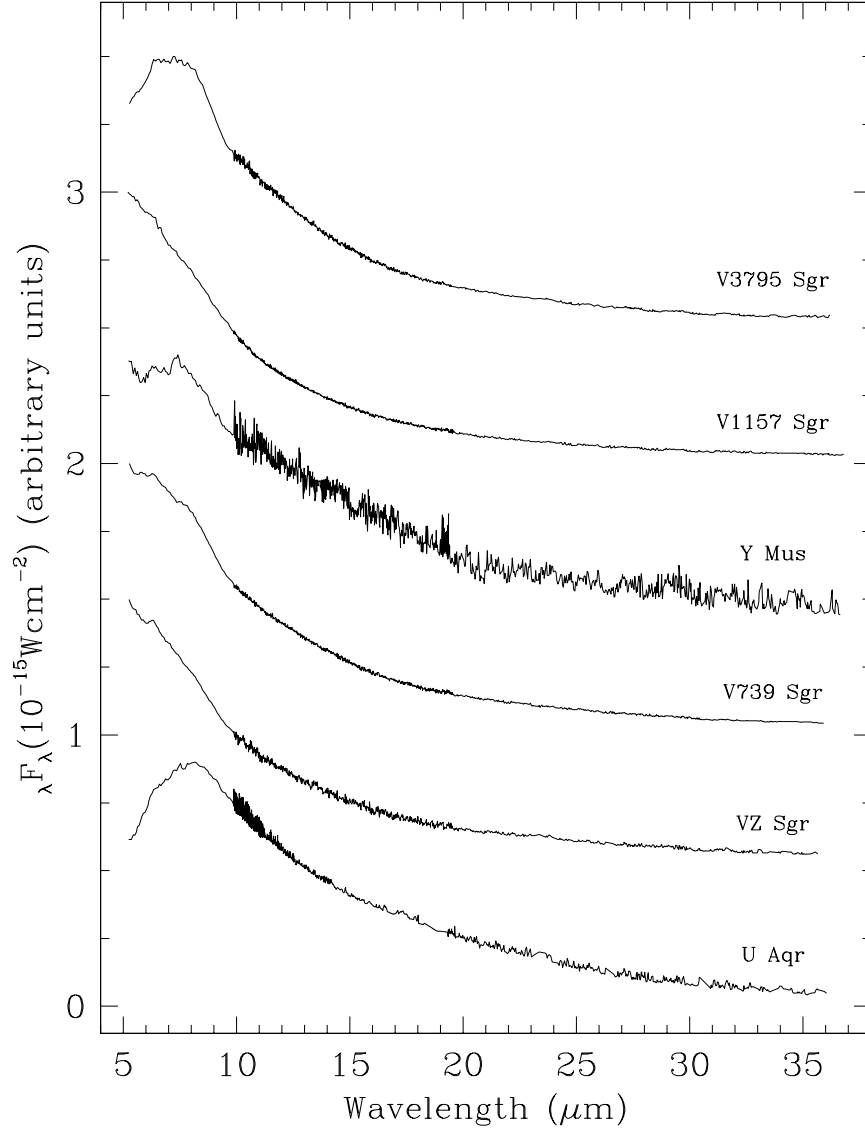


Fig. 2.— Spitzer/IRS reduced spectra over the full wavelength range $\sim 5\text{--}37 \mu\text{m}$ for V3795 Sgr, V1157 Sgr, Y Mus, V739 Sgr, VZ Sgr, and U Aqr. Note that the spectra are normalized and displaced for clarity.

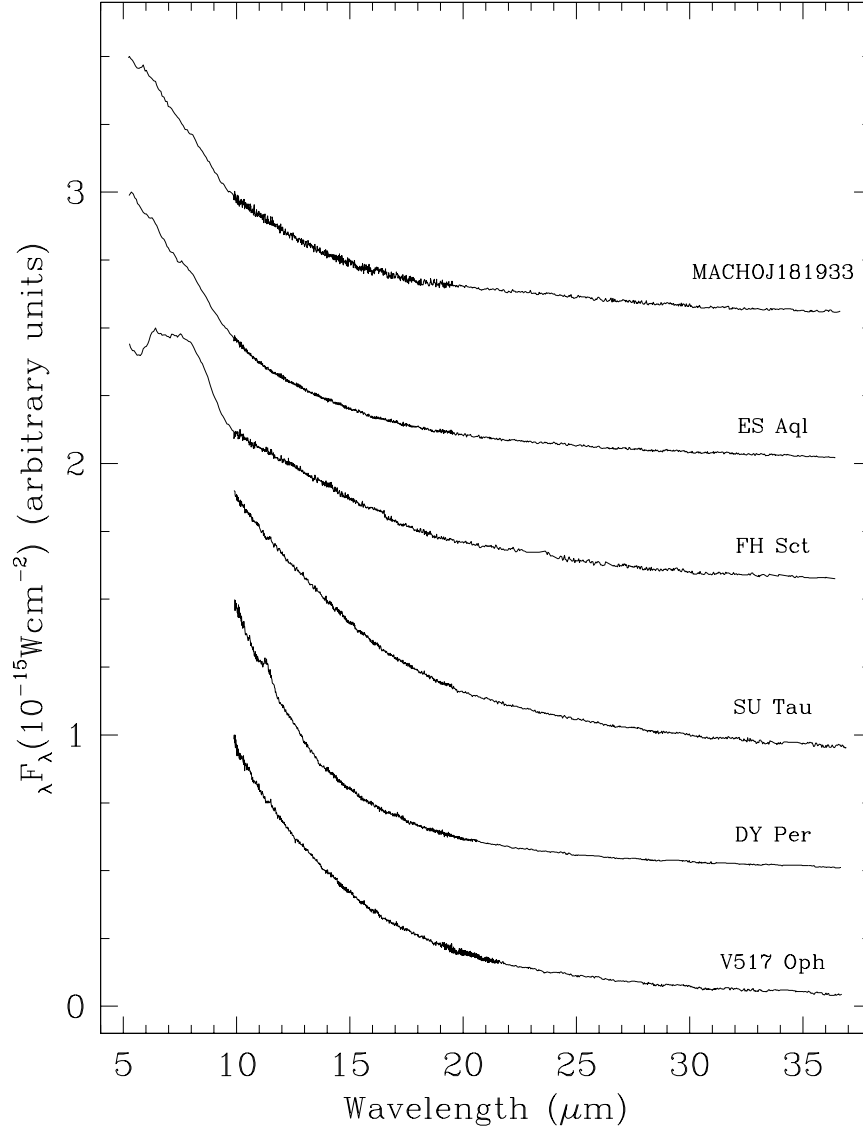


Fig. 3.— Spitzer/IRS reduced spectra over the full wavelength range $\sim 5\text{--}37 \mu\text{m}$ for MACHOJ181933, ES Aql, FH Sct, SU Tau, DY Per, and V517 Oph. Note that the spectra are normalized and displaced for clarity.

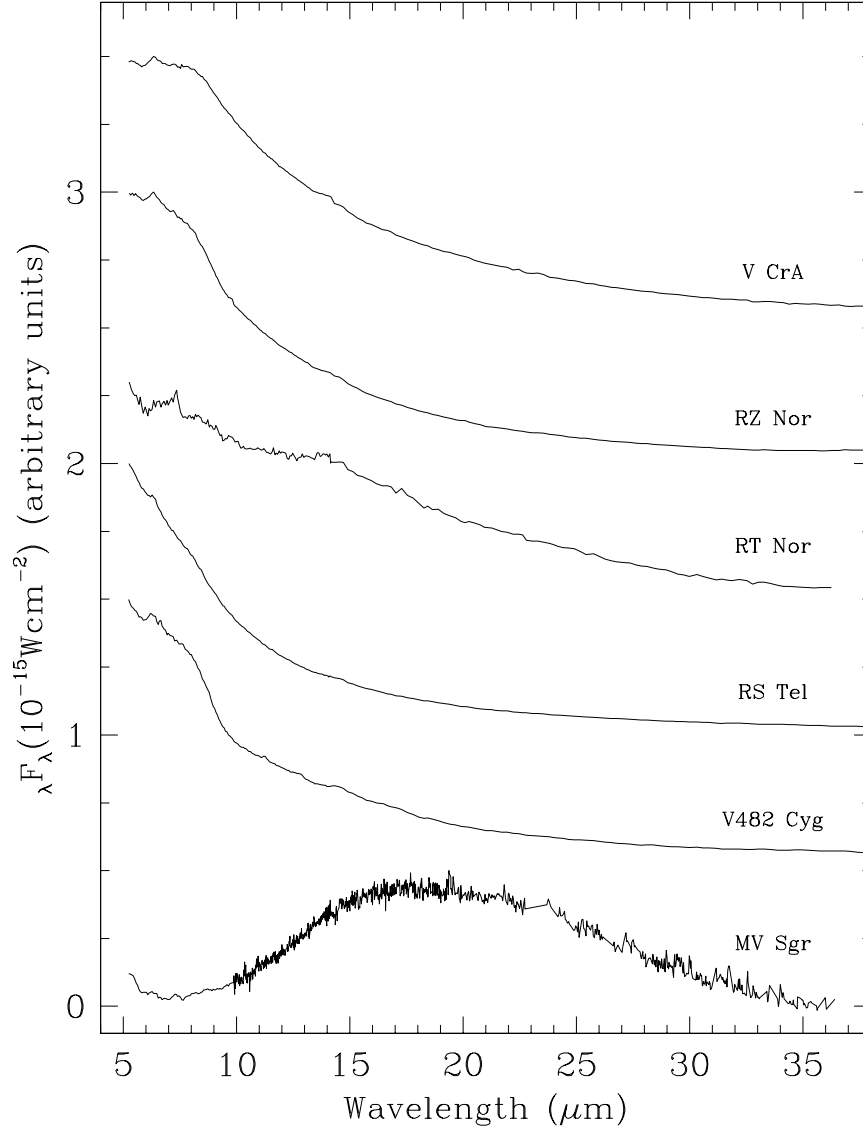


Fig. 4.— Spitzer/IRS reduced spectra over the full wavelength range $\sim 5\text{--}37 \mu\text{m}$ for V CrA, RZ Nor, RT Nor, RS Tel, V482 Cyg, and MV Sgr. Note that the spectra are normalized and displaced for clarity.

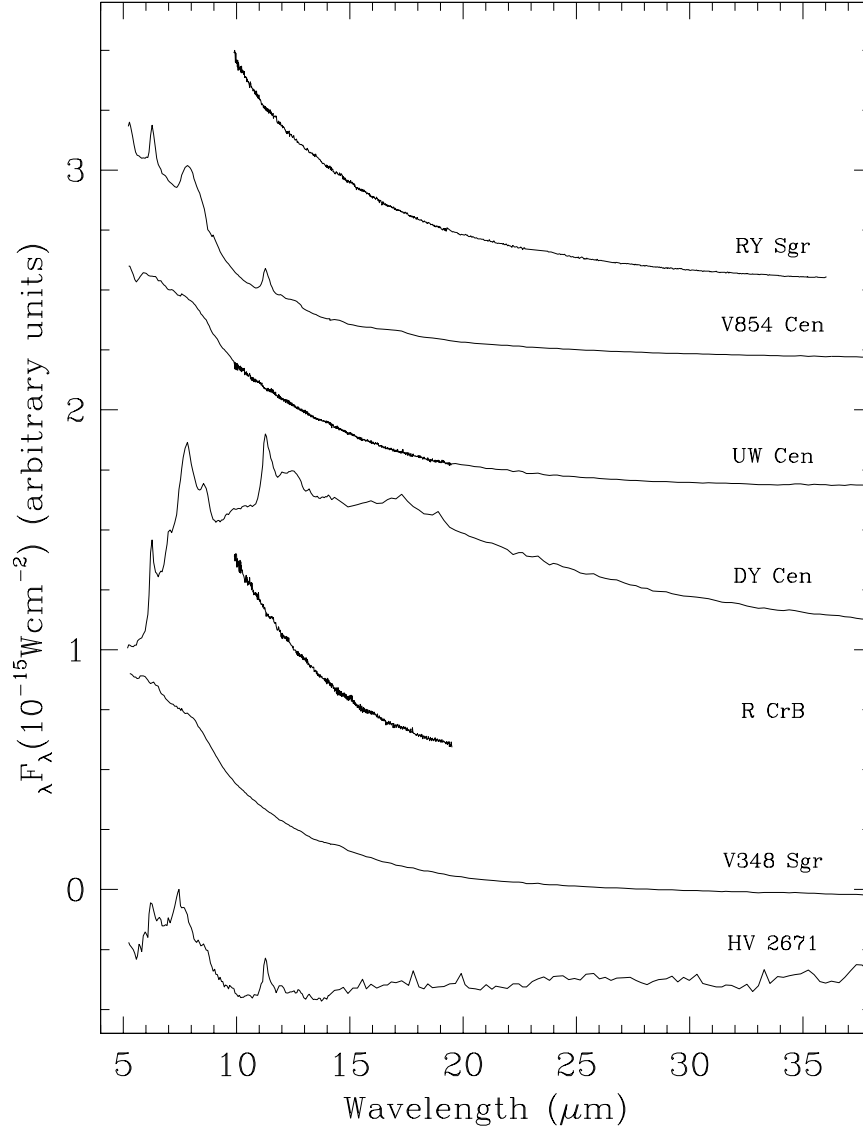


Fig. 5.— Spitzer/IRS reduced spectra over the full wavelength range $\sim 5\text{--}37 \mu\text{m}$ for RY Sgr, V854 Cen, UW Cen, DY Cen, R CrB, V348 Sgr, and HV 2671. Note that the spectra are normalized and displaced for clarity.

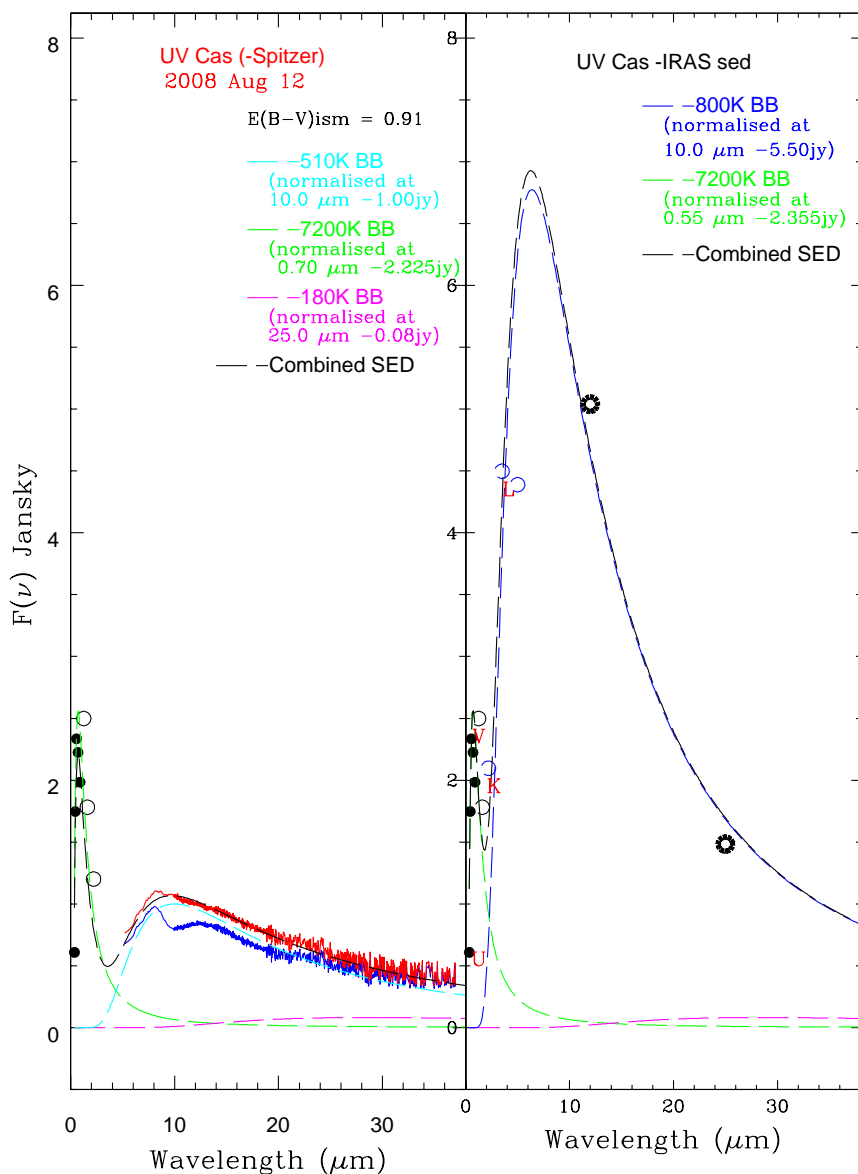


Fig. 6.— Blackbody fits for UV Cas. The lefthand panel shows a fit to the stellar fluxes computed from reddening-corrected UBVRI (UBV: Fernie et al. 1972; RI: this work) (black dots), 2MASS JHK (black open circles), and the Spitzer spectrum (corrected for interstellar reddening, in red). The observed Spitzer spectrum (in blue) and the blackbody temperatures are also shown. The righthand panel shows a fit to the stellar UBVRI and 2MASS JH fluxes and IRAS 12 μm and 25 μm fluxes with, in addition, the KLM fluxes (blue open circles) estimated from Bogdanov et al. (2010) for the IRAS epoch. Selected UVKL fluxes are labelled for convenience.

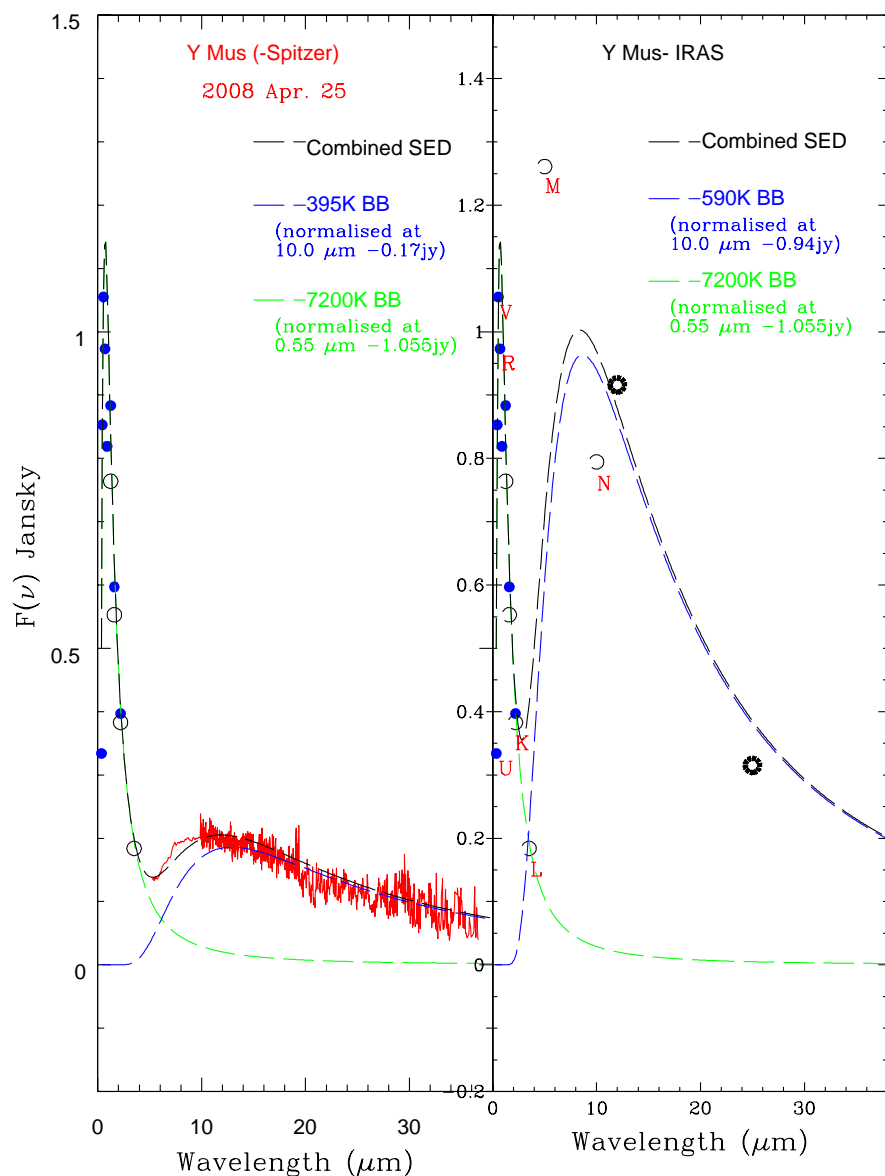


Fig. 7.— Blackbody fits for Y Mus. The lefthand panel shows a fit to the stellar fluxes computed from reddening-corrected UBVRI (Kilkenny et al. 1985) and JHK 2MASS photometry (blue dots) and JHKL (Feast et al. 1997) (black open circles), and the Spitzer spectrum (corrected for interstellar reddening, in red). The observed Spitzer spectrum (in blue) and the blackbody temperatures are also shown. The righthand panel shows a fit to the same stellar UBVRIJHK photometric fluxes and IRAS 12 μm and 25 μm fluxes with, in addition, fluxes at M and N from Kilkenny & Whittet (1984). Selected UVRKLMN fluxes are labelled for convenience.

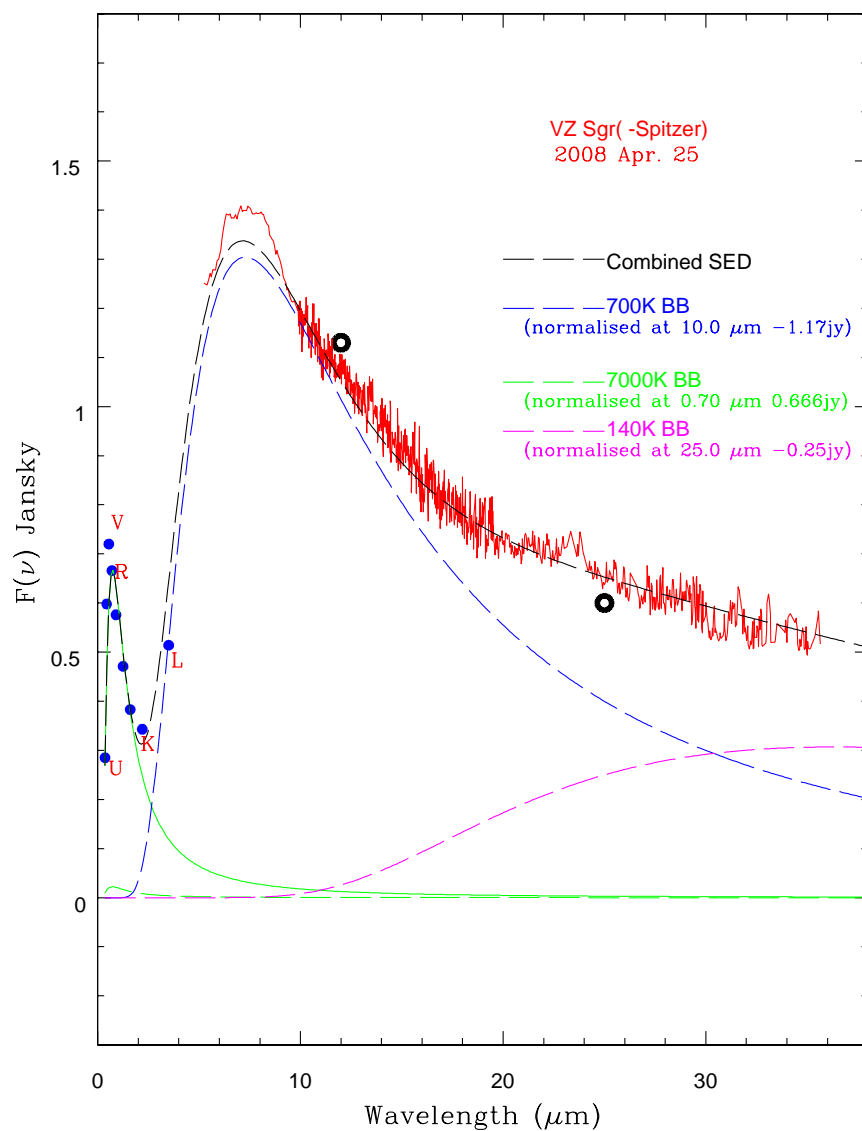


Fig. 8.— Blackbody fits for VZ Sgr. Reddening-corrected ground-based photometry at UBVRIJHKL (Kilkenny et al. 1985; Feast et al. 1997) and the Spitzer spectrum (in red) are fitted with a stellar (7000 K) blackbody and dust blackbodies at 700 K and 140 K. Note that the correction for interstellar reddening is negligible for VZ Sgr with $E(B-V)=0.3$ (see text). IRAS 12 μm and 25 μm fluxes are also shown and straddle the Spitzer spectrum. Selected UVRKL fluxes are labelled for convenience.

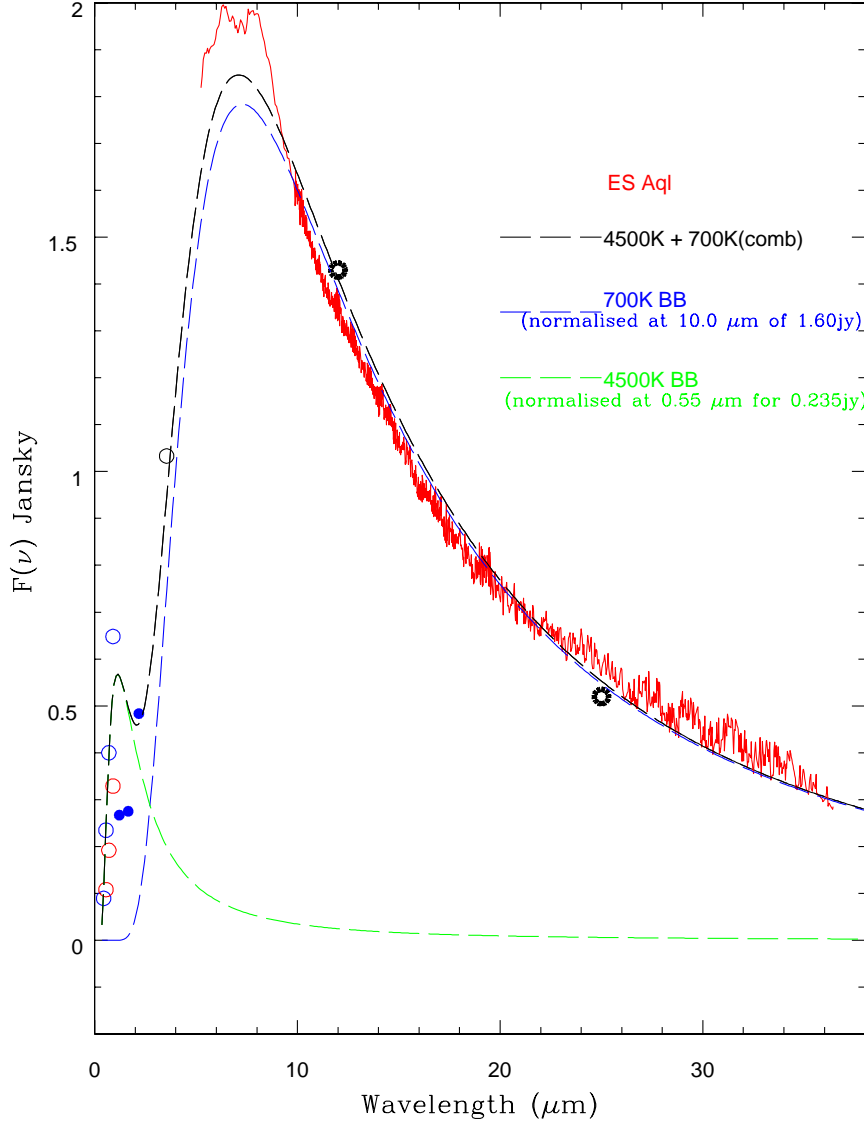


Fig. 9.— Blackbody fits for ES Aql. Reddening-corrected VRI ground-based photometry (red open circles) and the Spitzer spectrum (corrected for interstellar reddening, in red) are fitted with a stellar (4500 K) blackbody and a dust blackbody at 700 K. IRAS 12 μm and 25 μm fluxes are shown and straddle the Spitzer spectrum. Reddening-corrected BVRIJHKL fluxes (see text) correspond to our VRI ground-based observations (red open circles, Table 2), BVRI at maximum light (blue open circles), 2MASS JHK (blue dots) and L magnitude (black open circle).

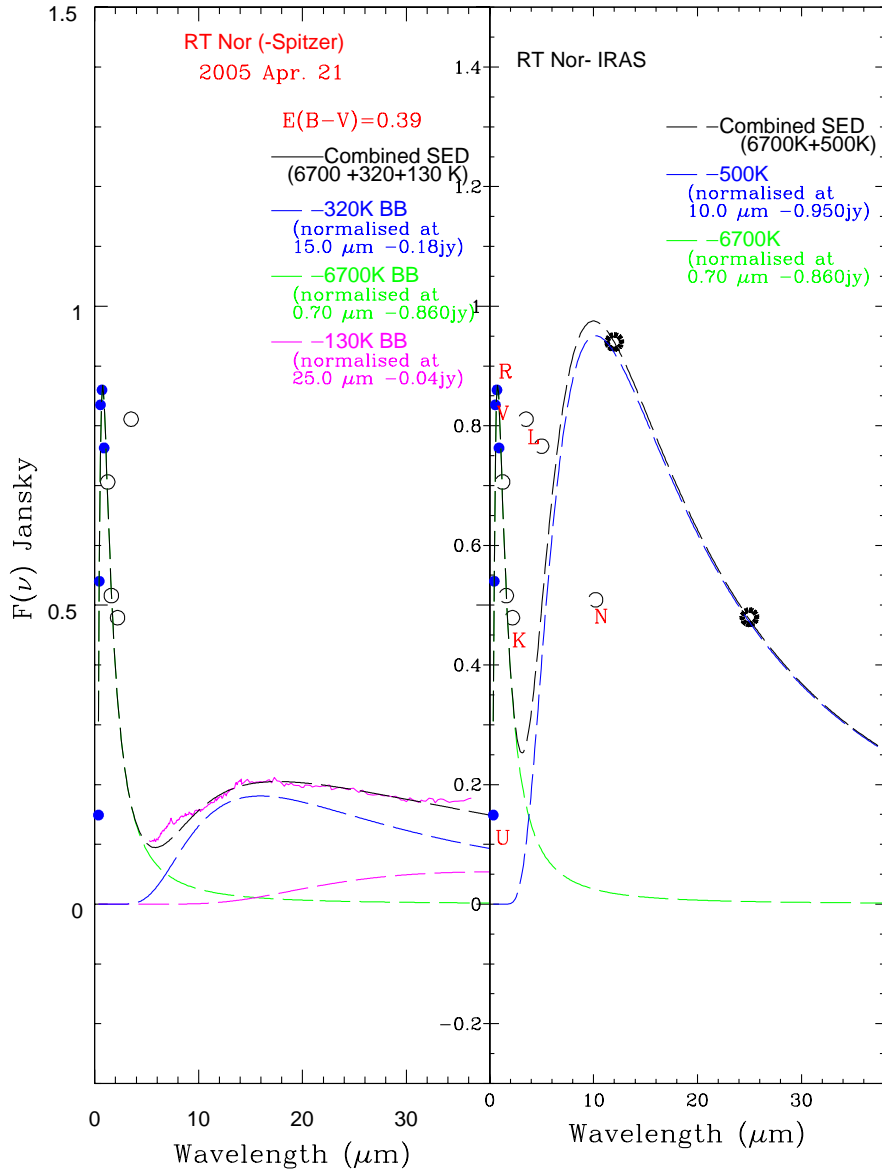


Fig. 10.— Blackbody fits for RT Nor. The lefthand panel shows a fit to the stellar fluxes computed from reddening-corrected UBVRI (Kilkenny et al. 1985) (blue dots) and JHKL (Feast et al. 1997) (open circles) and the Spitzer spectrum (in red) with the blackbody temperatures shown on the panel. Note that the correction for interstellar reddening is negligible for RT Nor with $E(B-V)=0.39$ (see text). The righthand panel shows a fit to the same stellar UBVRIJHKL photometric fluxes and IRAS $12\ \mu\text{m}$ and $25\ \mu\text{m}$ fluxes with, in addition, fluxes at M and N from Kilkenny & Whittet (1984). Selected UVRKLN fluxes are labelled for convenience.

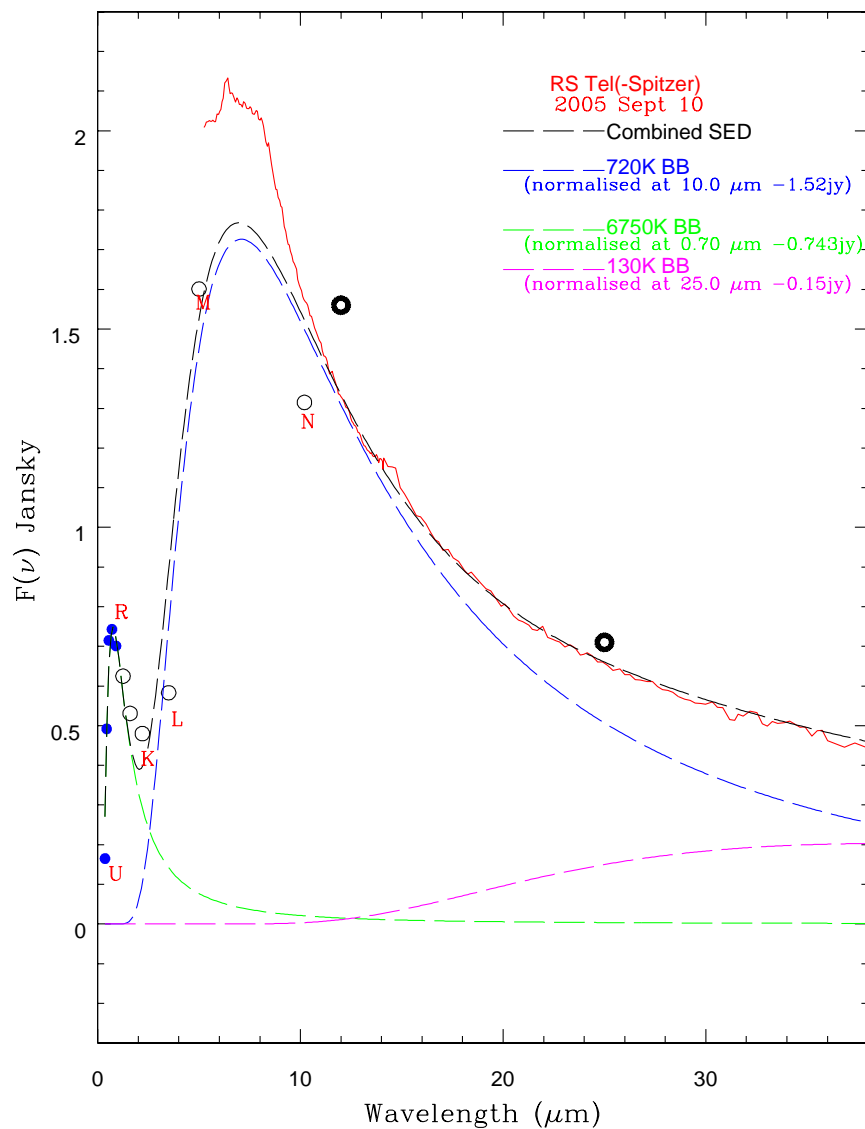


Fig. 11.— Blackbody fits for RS Tel. Ground-based reddening-corrected photometry at UBVRIJHKL (Kilkenny et al. 1985; Glass 1978; see text) and the Spitzer spectrum (in red) are fitted with a stellar (6750 K) blackbody and dust blackbodies at 720 K and 130 K. Note that the correction for interstellar reddening is negligible for RS Tel with $E(B-V)=0.17$ (see text). IRAS 12 μm and 25 μm fluxes and MN from Kilkenny & Whittet (1984) are also shown. Selected URKLMN fluxes are labelled for convenience.

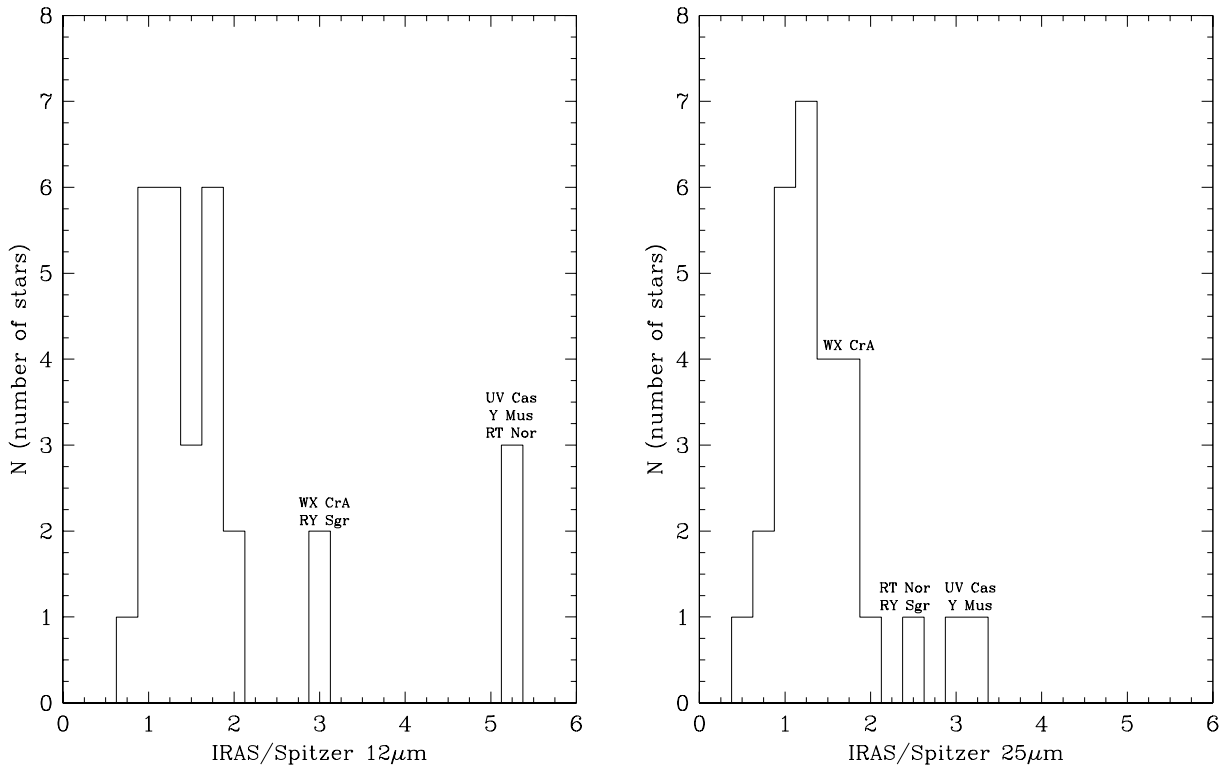


Fig. 12.— Histograms of the IRAS/Spitzer flux ratios. Left panel - fluxes at 12 μm . Right panel - fluxes at 25 μm . Fluxes are uncorrected for interstellar reddening. Color corrections have not been applied to the IRAS fluxes. Five outliers are identified.

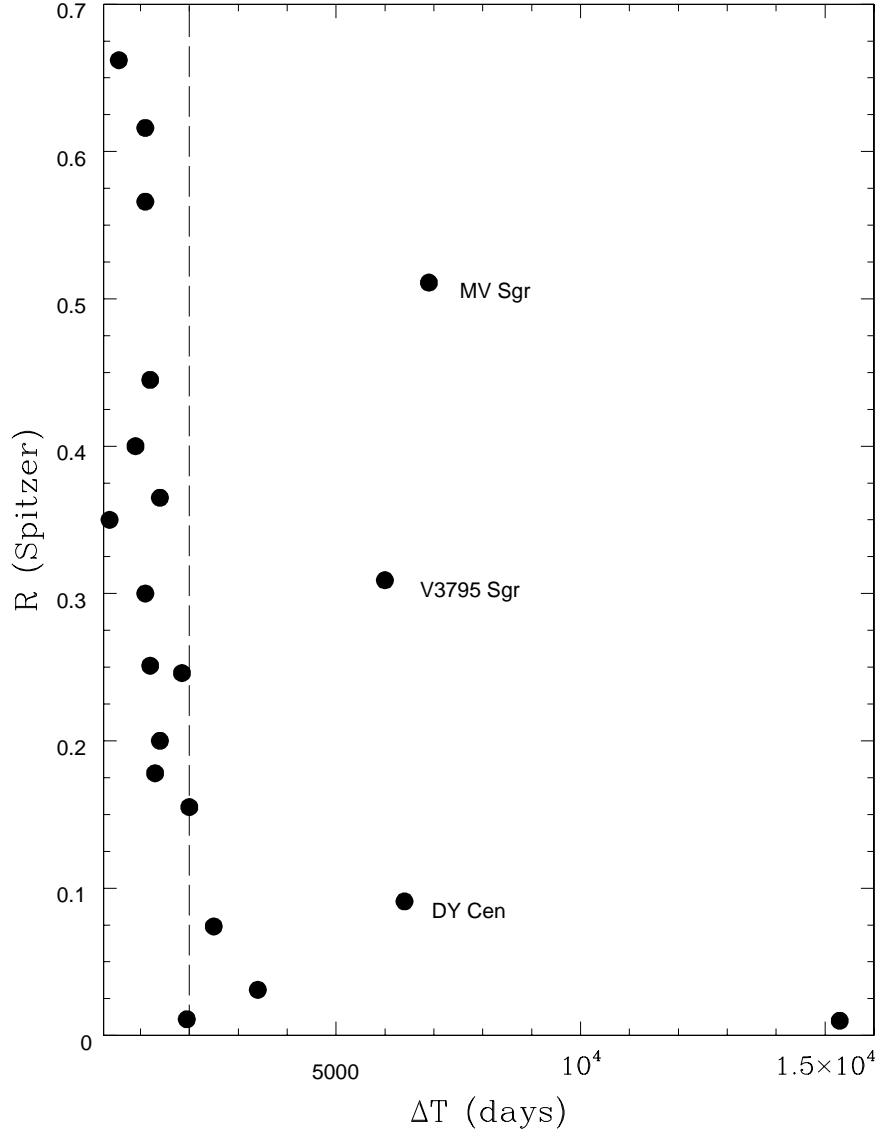


Fig. 13.— Spitzer Covering factor R versus the inter-fade period ΔT . The dashed vertical line marks the point $\Delta T=2000$ days discussed in the text. Note that UV Cas with the longest $\Delta T=25500$ days and a very low $R=0.035$ is not shown for clarity.

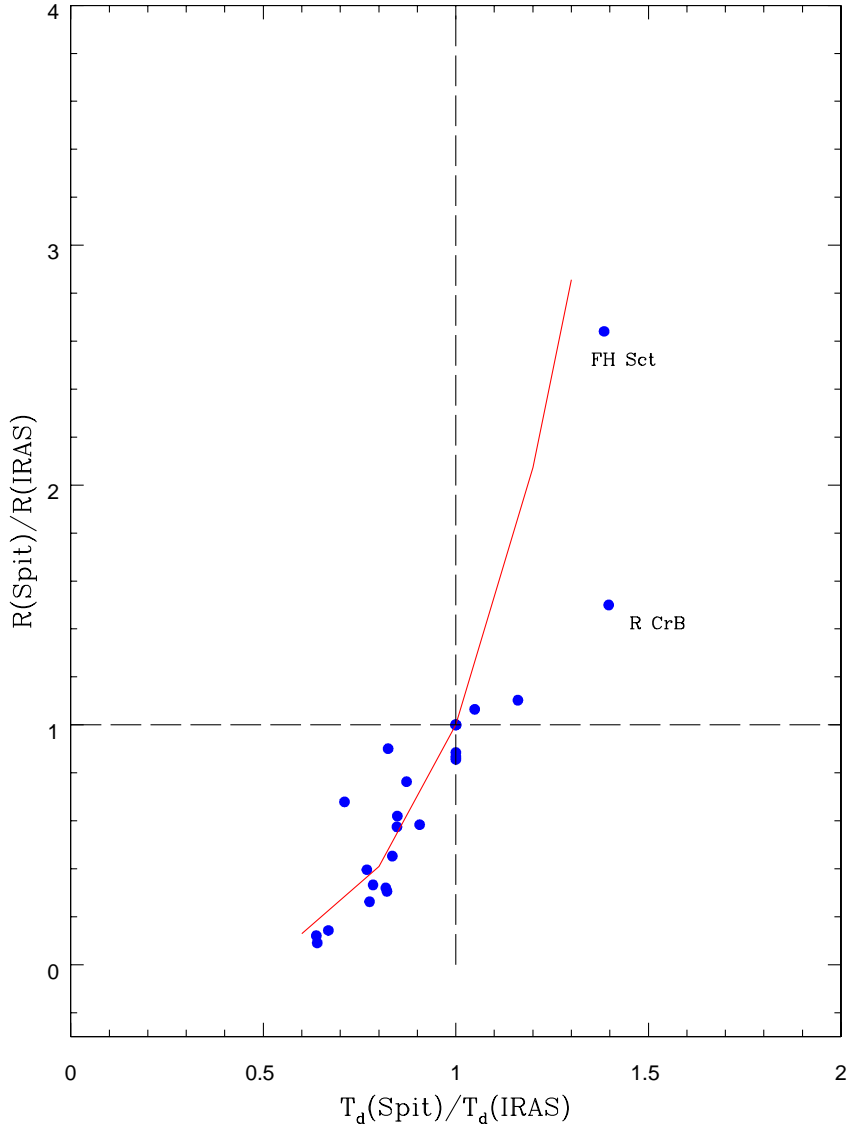


Fig. 14.— The ratio of the Spitzer to IRAS blackbody dust temperatures versus the ratio of the Spitzer to IRAS covering factors. The solid line is the simple prediction discussed in the text.

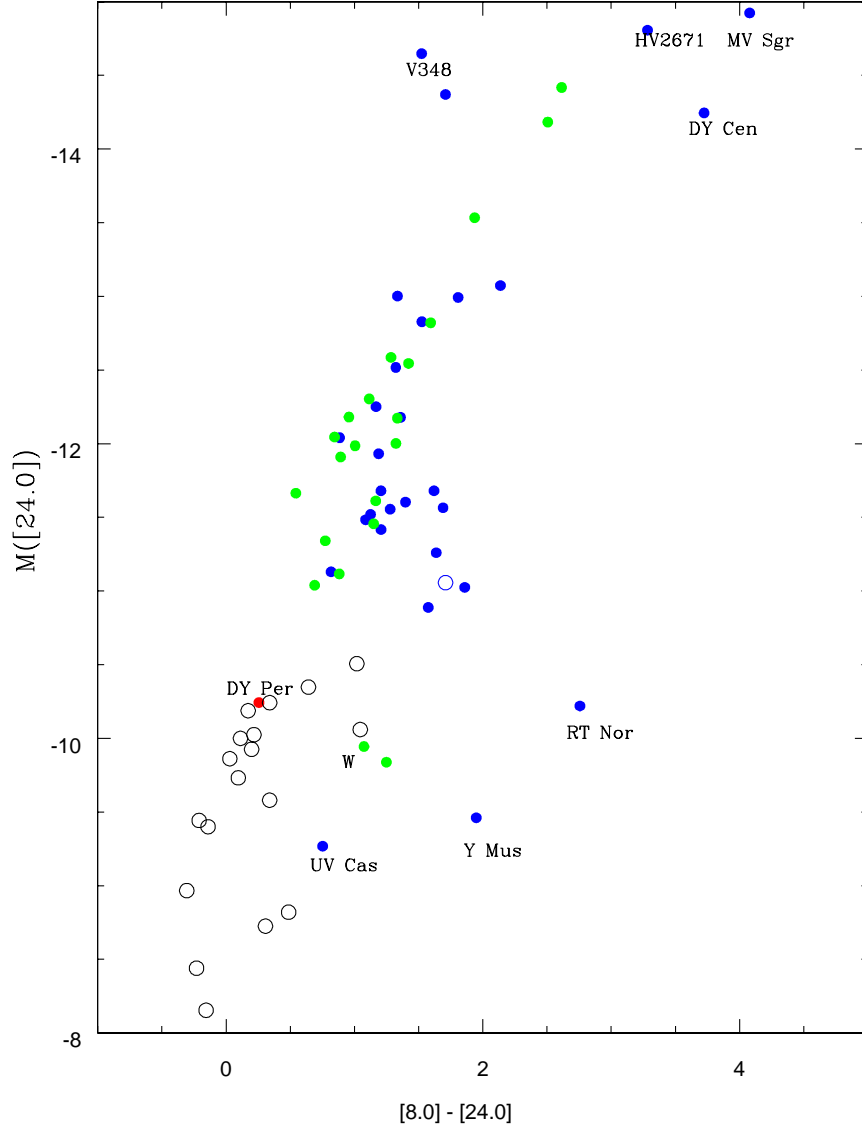


Fig. 15.— $[24.0]\mu\text{m}$ absolute magnitude versus the $[8.0]-[24.0]$ color index for our sample of Galactic RCBs (blue dots) in comparison with LMC RCBs (green dots) and LMC DY Per-like stars (black open circles). Hot RCBs (V348 Sgr, DY Cen, MV Sgr and HV 2671) are located towards the $[24.0]\mu\text{m}$ high luminosity end and are labelled. The three RCB stars (UV Cas, Y Mus, and RT Nor) showing remarkably low $[24.0]\mu\text{m}$ magnitudes are also labelled. Note that DY Per itself and W Men are also marked with a red dot and the letter ‘W’, respectively.